

Distance Ladder

I. Aretxaga

2020

Distance Ladder

Primary Indicators:

- can be measured in nearby galaxies
- small dispersion around a well defined mean
- can be calibrated through geometrical means

e.g. **cepheids**, novas, RR Lyrae, BA supergiants, eclipsing binaries,

...

Secondary, tertiary, ... indicators:

- are calibrated through primary, secondary... indicators

e.g. **Type Ia supernovae**, **Tully-Fisher**, **D_n-σ**, brightest stars, planetary nebulae, ...

Primary Indicators: Cepheids (~20 Mpc)

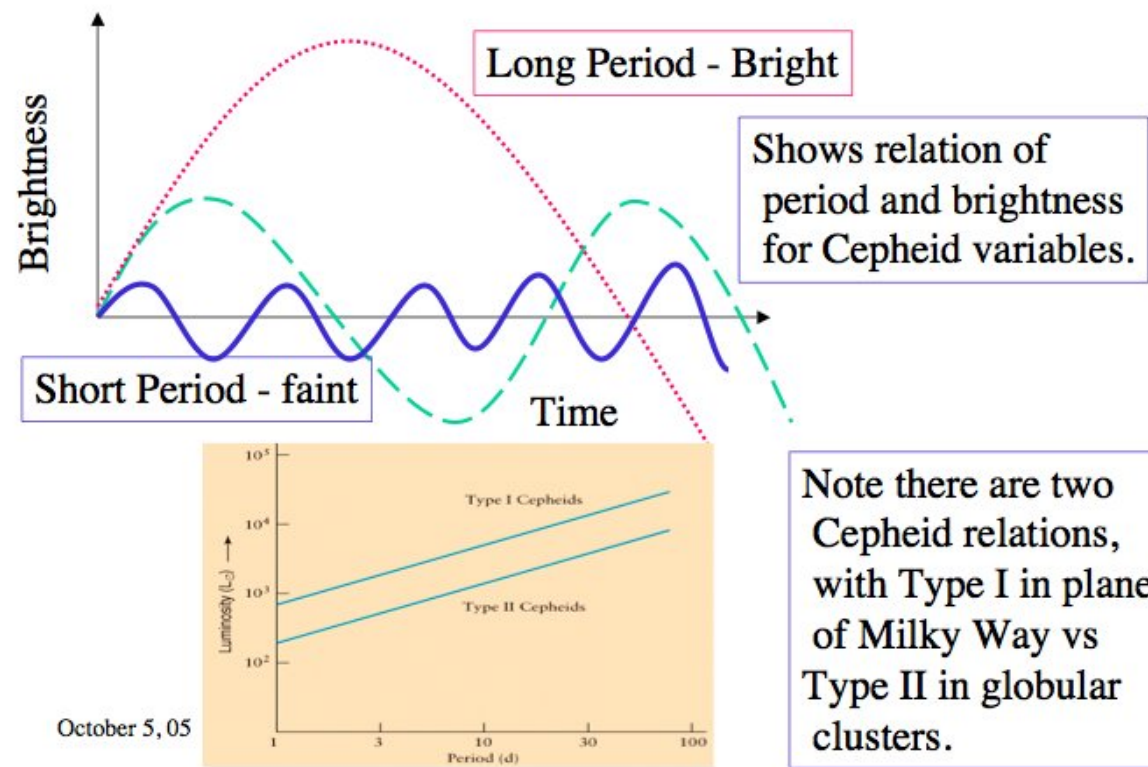
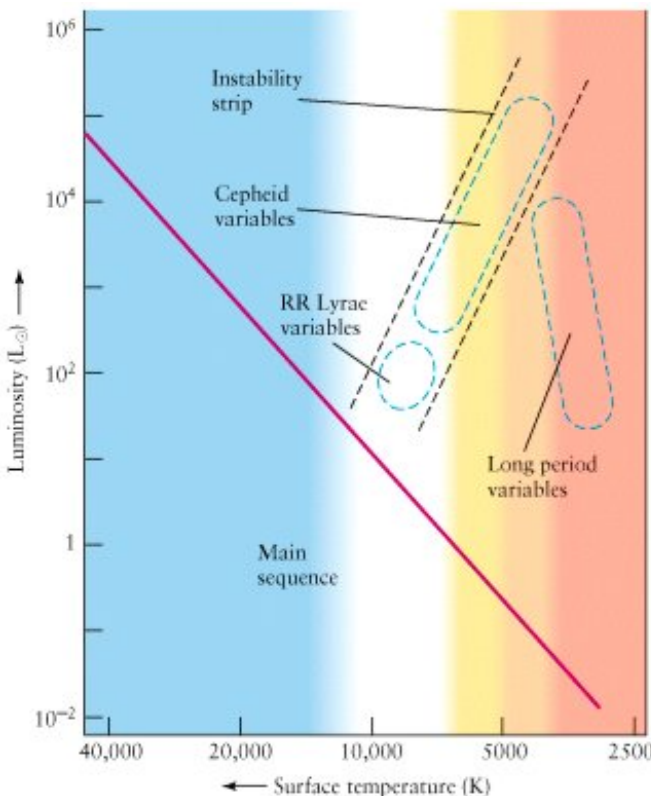
Cepheid stars are long-period variables (\sim 1-100 days) and they display a tight luminosity-period linear relationship (better than 10% precision), which is weakly dependent on metallicity.

$$M_V = -2.80 \log P_d - (1.43 \pm 0.1)$$

(Feast & Catchpole 1997)

$$\delta(m - M)_0 = -0.24 \pm 0.16$$

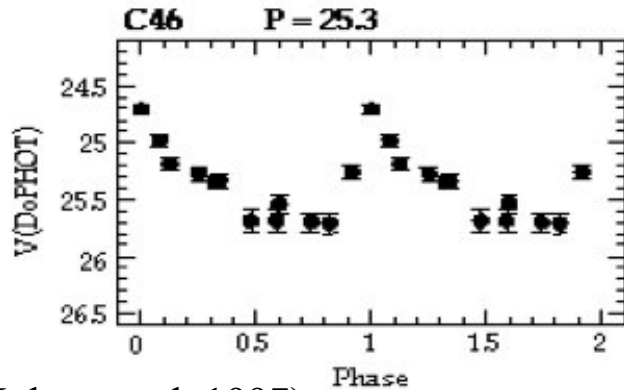
(Kennicutt et al. 1998) Metal rich brighter



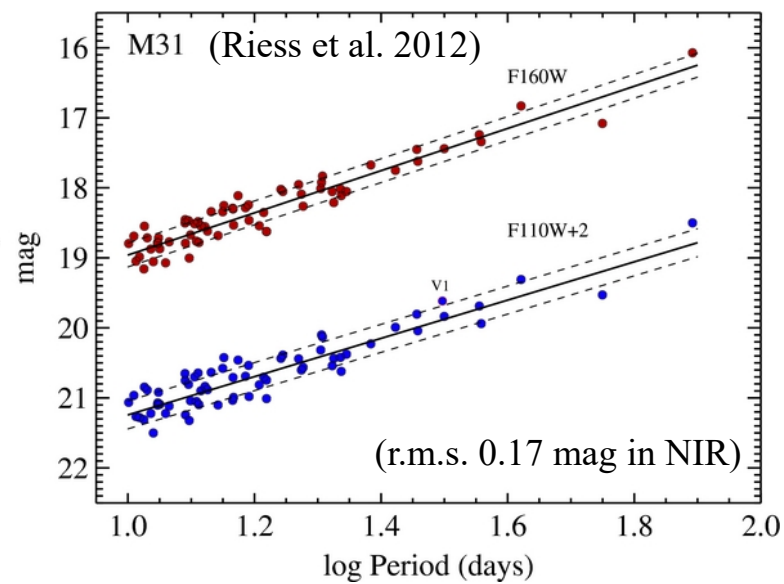
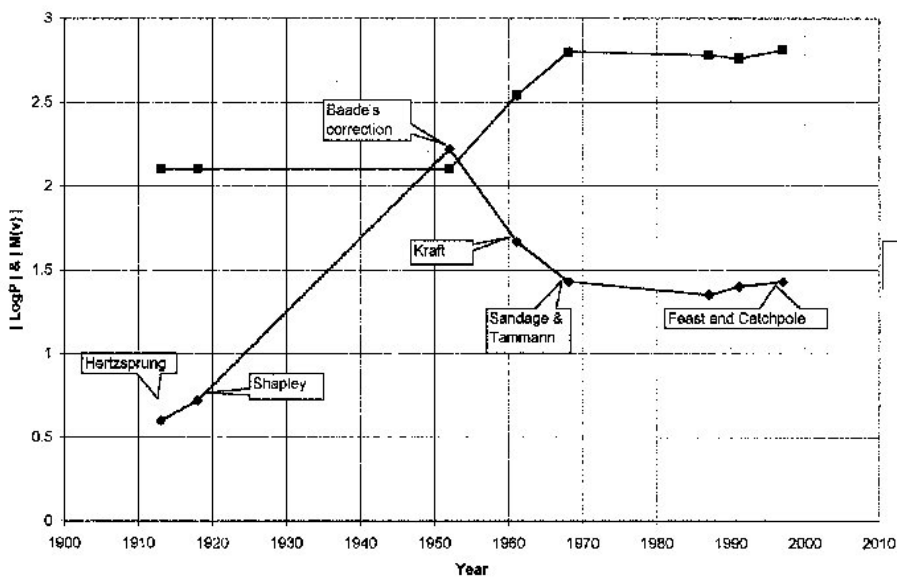
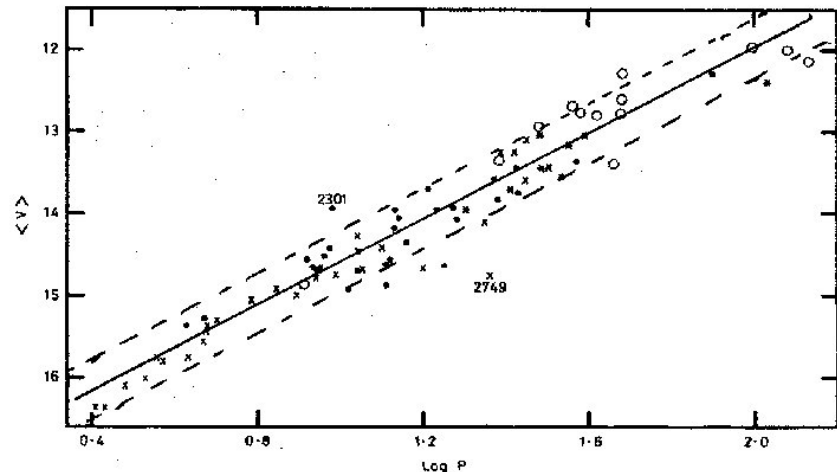
Shows relation of period and brightness for Cepheid variables.

Note there are two Cepheid relations, with Type I in plane of Milky Way vs Type II in globular clusters.

Primary Indicators: Cepheids (~20 Mpc)



(Kelson et al. 1997)



(Allen 2001: <http://www.institute-of-brilliant-failures.com/index.htm>)

Primary Indicators: Cepheids (\sim 20 Mpc)

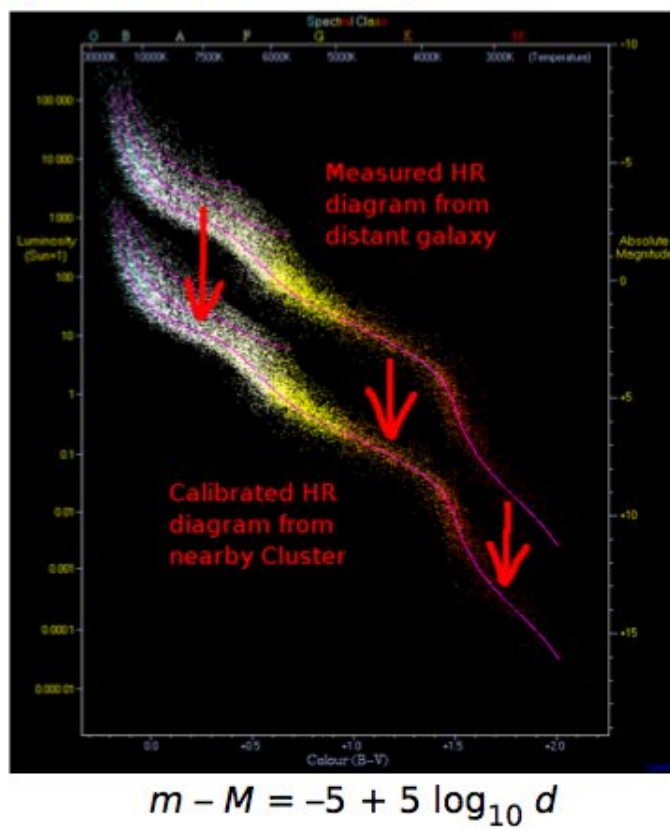
H_0 Key Project

- ◆ What do we do with all of these distances?
- ◆ H_0 Key Project – started in 1990, final results 2001!
 - Observe Cepheids in \sim 18 spiral galaxies to test the universality of the Cepheid P-L relation and greatly improve calibration of other distance indicators which generally rest on one or two local group galaxies
 - Their Cepheid P-L relation zeropoint is tied directly to the distance to the LMC (largest source of error in current estimate of H_0 !)
 - Combining different estimators, they find $H_0 = 72 \pm 3$ (random) ± 7 (systematic) km/s/Mpc !
 - But note that it's not over yet as some people disagree with their adopted value for the distance to the LMC ...
 - ... and other methods give different answers!

Other primary Indicators: main sequence (~10 kpc)

Main Sequence Fitting

Most stars are located on the Main Sequence in the HR Diagram:



Other primary Indicators:

Eclipsing binaries: Uses Kepler's 3rd law, Stefan-Boltzmann relationship and assumes a M/L.

Novas: relationship between maximum Luminosity and decay time

RR Lyrae: constant magnitude and color.

BA Supergiant Stars: based on the Barbier & Chalone classification method, which measures the Balmer break.

Secondary Indicators: type Ia SNe (~ 4 Gpc)

Not really a standard candle, but a candle that can calibrated
Advantages: - bright

- small dispersion (<0.3 mag)
- small corrections for absorption
- they occur in all Hubble types

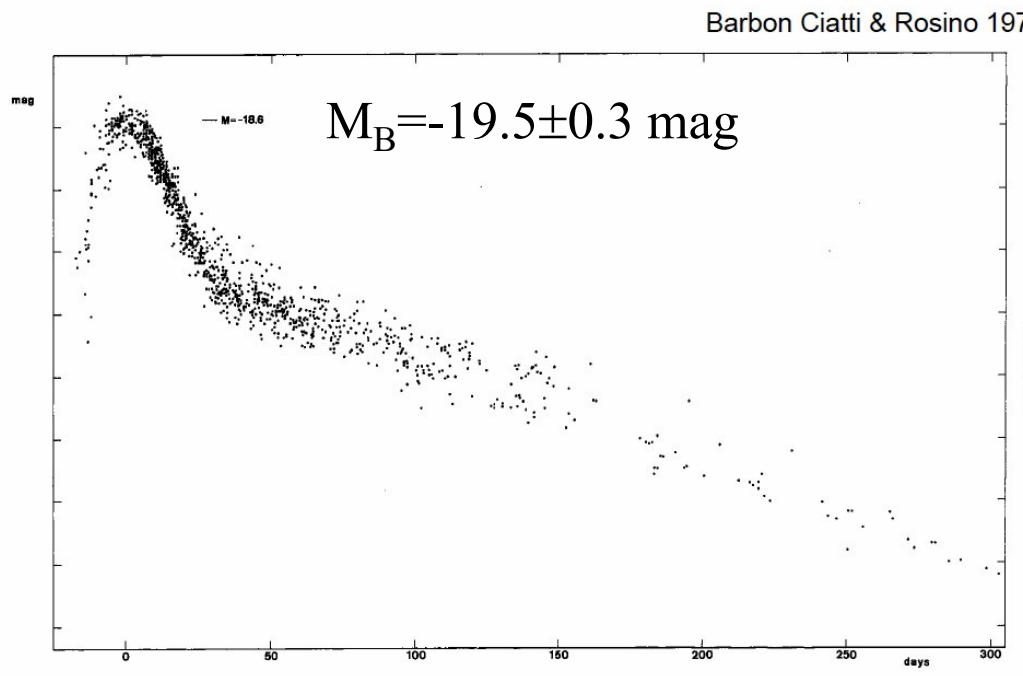
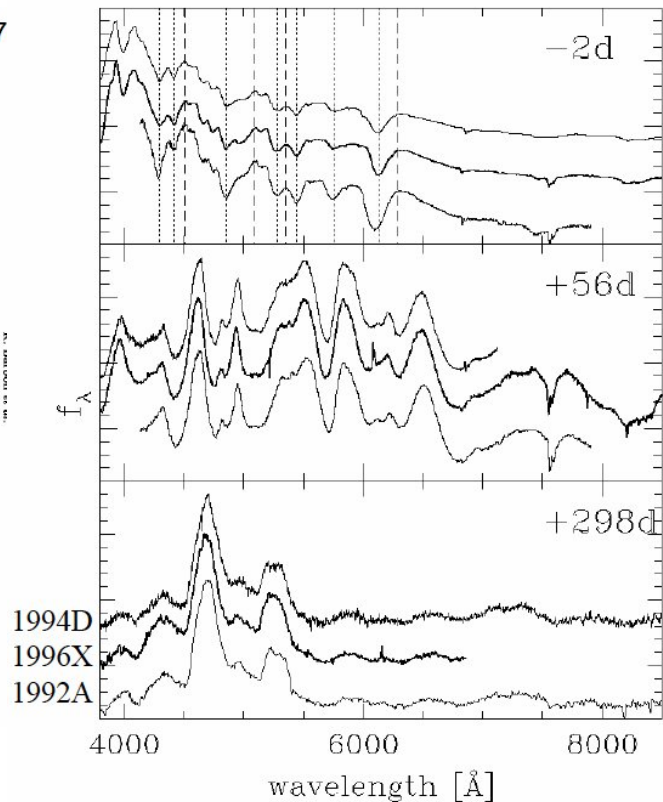
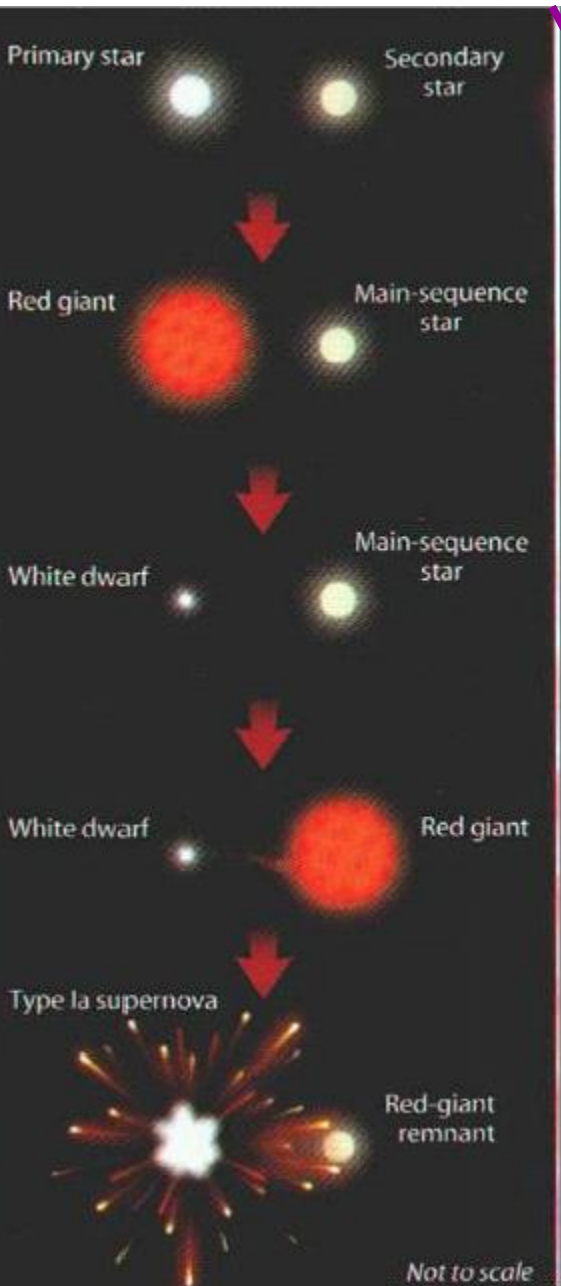


Fig. 1. Average blue light curve, obtained by the fitting (as explained in the text) of the observations of 38 type I supernovae (see Table 1). One magnitude intervals are marked on the ordinates



SNe: taxonomy



Early Spectra:

SN I
Si/ No Si

SN Ia

1985A
1989B

No Hydrogen / Hydrogen

SN II

~3 mos. spectra
He dominant/H dominant

He poor/He rich

SN Ic

1983I
1983V

SN Ib

1983N
1984L

SN IIb

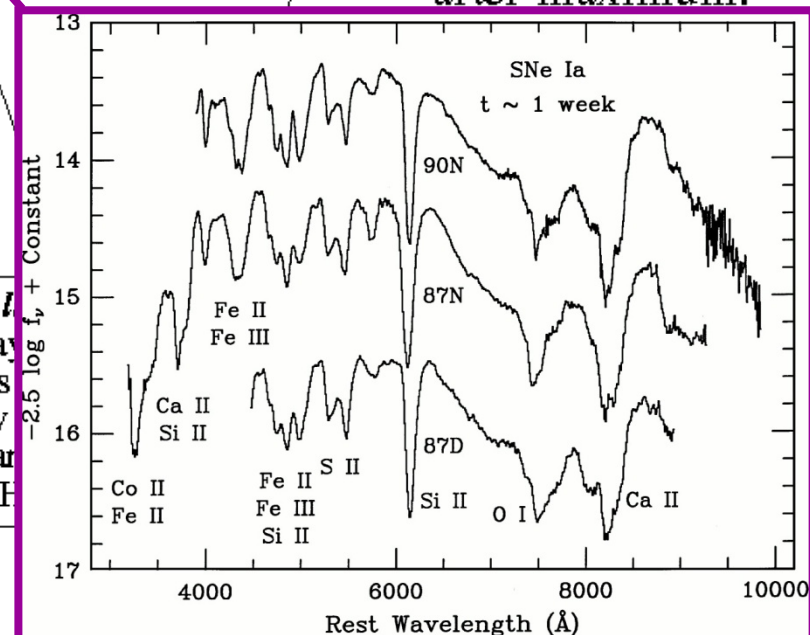
1993J
1987K

Believed to originate from *deflagration* or *detonation* of an *accreting white dwarf*.

Theory

Core Col
Outer Lay
by winds
or binary
Ib: H mar
Ic: H & H

(Filippenko 1997)



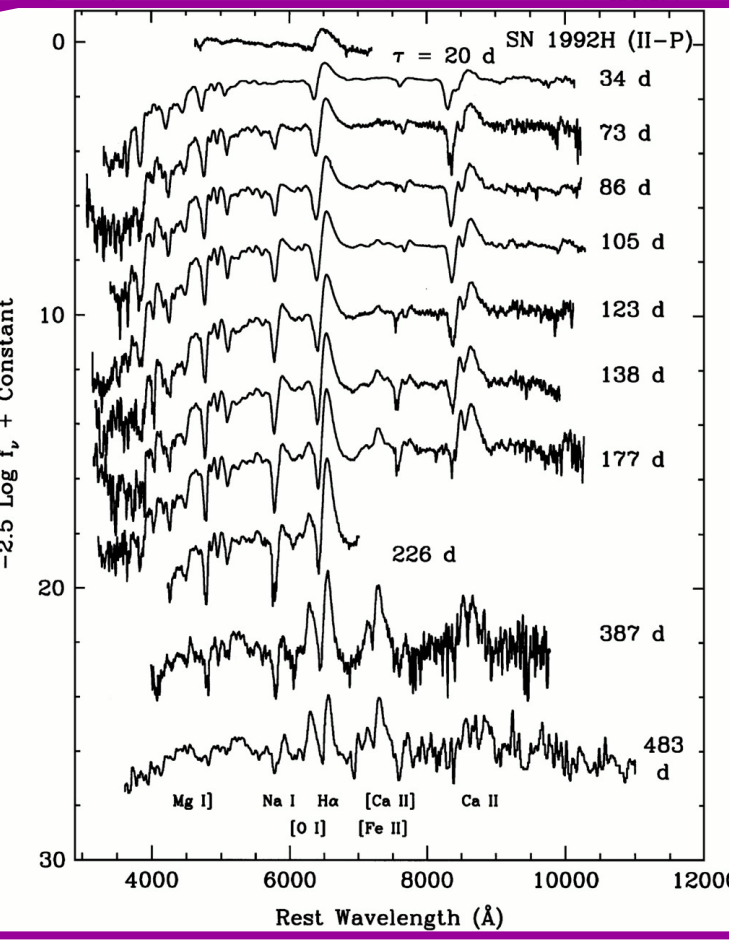
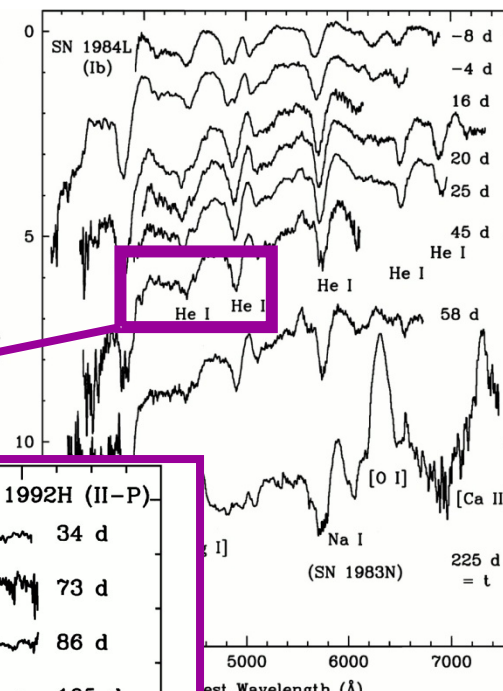
SNe: taxonomy



Early Spectra:

No Hydrogen

SN I
Si/ No Si



Light Curve decay
after maximum:
Linear / Plateau

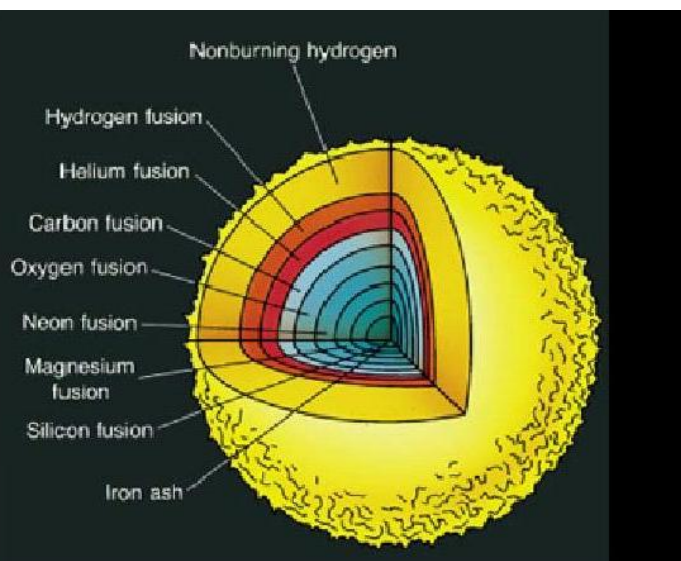
SN III

SN IIP

1980K
1979C

1987A
1988A
1969L

Core Collapse of
a massive progenitor
with plenty of H .



SNe: taxonomy



Early Spectra:

No Hydrogen / Hydrogen

SN I
Si/ No Si

SN II

~3 mos. spectra
He dominant/H dominant

SN Ia

1985A
1989B

He poor/He rich

SN Ic

983I
983V

SN Ib

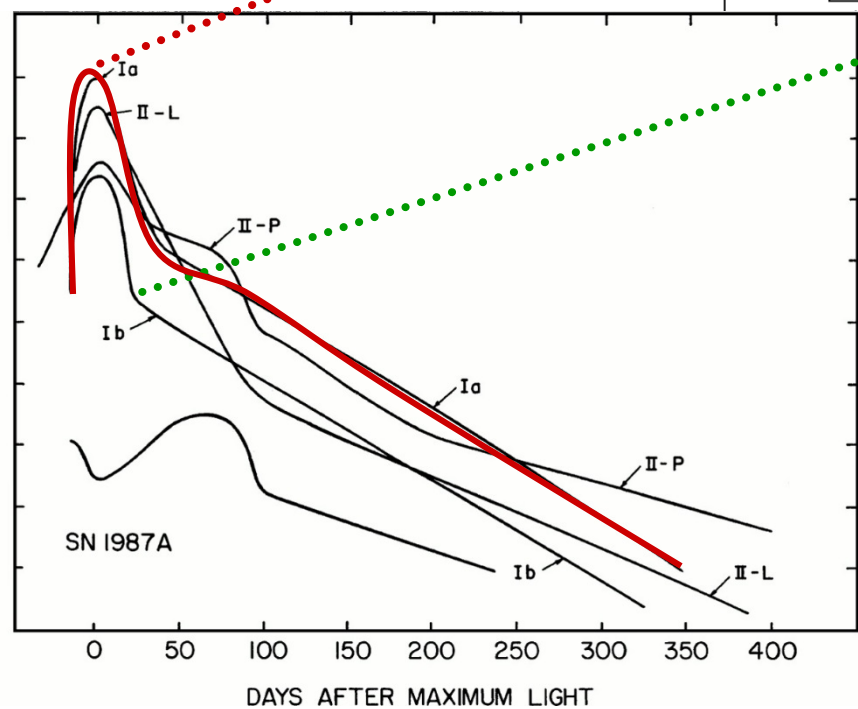
1983N
1984L

SN IIb

1993J
1987K

“Normal” SNII

Light Curve decay
after maximum:
Linear / Plateau



originate
at the
bottom
of an
white dwarf.

Core collapse.
Most (NOT all)
H is removed during
evolution by
tidal stripping.

Core Collapse.
Outer Layers stripped
by winds (*Wolf-Rayet Stars*)
or binary interactions
Ib: H mantle removed
Ic: H & He removed

SN III
1980K
1979C

SN IIP
1987A
1988A
1969L

Core Collapse of
a massive progenitor
with plenty of H .

Secondary Indicators: type Ia SNe (~ 4 Gpc)

Not really a standard candle, but a candle that can be calibrated

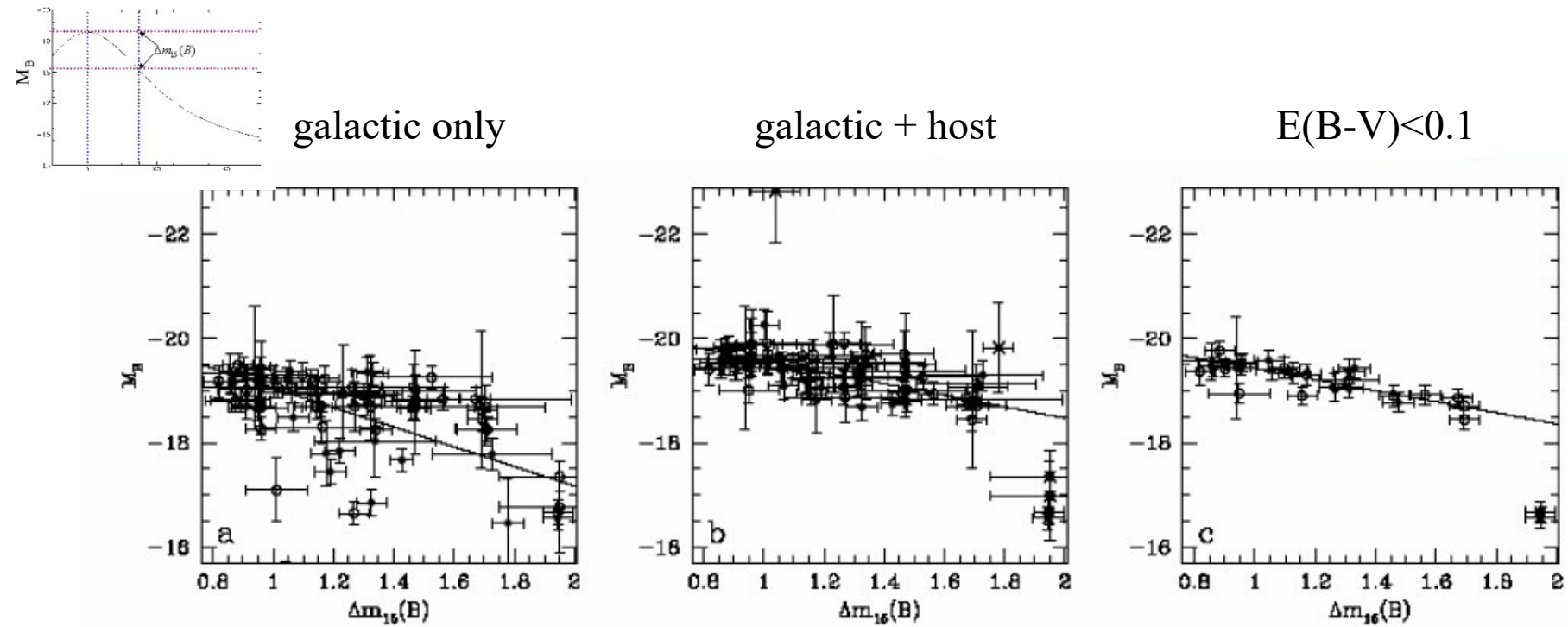


Figure 5. M_B versus $\Delta m_{15}(B)$ relation; filled circles indicate objects whose distances are given by Tully's catalogue, open symbols are objects whose distances are calculated from their recession velocity. The linear fit is weighted in both axes (Press 1992). a: Only galactic reddening correction applied. Number of objects used for the linear fit $n=73$, dispersion $\sigma = 0.83$. b: Both Galactic and host galaxy reddening corrections applied. The outliers, marked with a cross, are (from left to right, from top to bottom): SN 1996ai, which is characterized by high and not well known reddening; SN 1986G, another highly reddened event; SN 1992K, 1999da, 1998de, 1991bg, which are peculiar sub-luminous events. The latters seem to form a separate class and do not fit the linear relation defined by all others. $n=67$, $\sigma = 0.31$. c: as the previous case but selecting only SNe with $E(B-V) < 0.1$ and small errors (< 0.2) in $\Delta m_{15}(B)$. $n=26$, $\sigma = 0.20$. $R_R = 3.5$.

(Hamuy et al. 1996)

Secondary Indicators: type Ia SNe (\sim 4Gpc)

Not really a standard candle, but a candle that can be calibrated

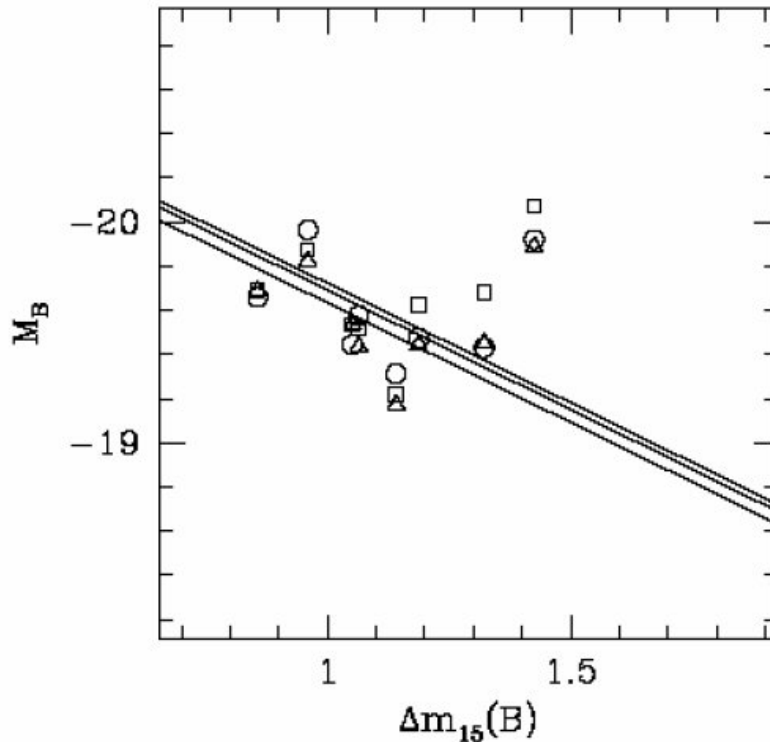


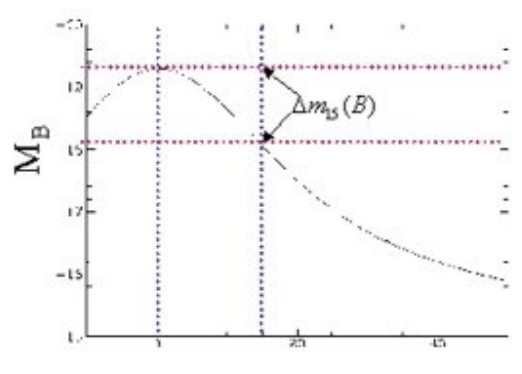
Figure 8. M_B versus $\Delta m_{15}(B)$ for 8 of the 9 SNe calibrated by Cepheids (SN 1960F has been excluded because colour information required to estimate the host galaxy extinction is not available). Circles: Distance modulus μ from Freedman et al. 2001; triangles: μ corrected assuming $\Delta Y/\Delta Z = 2.5$; square: μ corrected assuming $\Delta Y/\Delta Z = 3.5$. Solid lines are the best fits obtained with a fixed slope minimizing the deviation of the three sets of Cepheids calibrated SNe. The slope (1.082) is the same as in Fig. 5c.

Secondary Indicators: type Ia SNe (~ 4 Gpc)

$$M_B = a (\Delta m_{15}(B) - 1.1) + b$$

Table 1. Parameters of the $M_B = a(\Delta m_{15}(B) - 1.1) + b$ relation. From top to bottom: values obtained for case b, c (as in §2.3). From left to right: number of objects used for the correlation; R_B adopted; slope (error); zero point derived from three different assumptions on the metallicity PL relation (error); dispersion.

n	R_B	a	b			σ
			KP	$\Delta Y/\Delta Z = 2.5$	$\Delta Y/\Delta Z = 3.5$	
67	4.315	1.102 (0.147)	-19.613	-19.523	-19.582	(0.037) 0.31
67	3.5	1.092 (0.124)	-19.460	-19.399	-19.472	(0.031) 0.28
26	3.5	1.061 (0.154)	-19.455	-19.403	-19.476	(0.044) 0.20

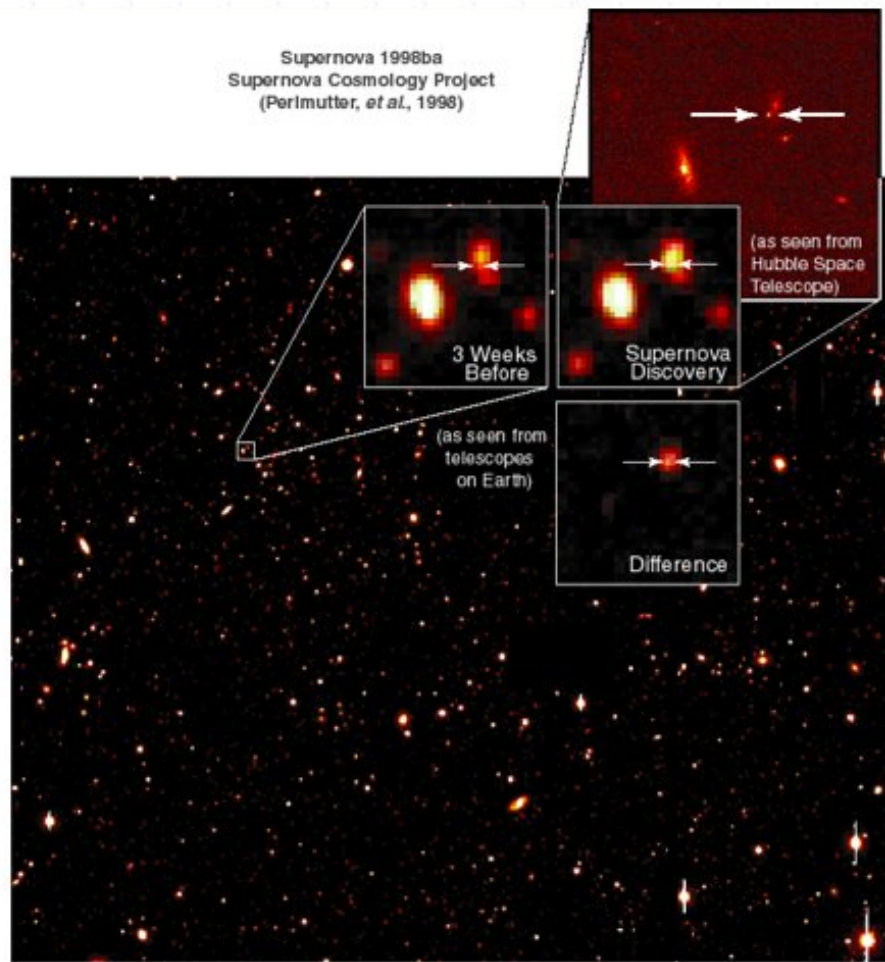


Hamuy et al. 1996, $b = -19.258 + 0.048$

Secondary Indicators: high-z SNe (~4Gpc)

Two teams doing high-z SN searches to measure cosmological parameters:

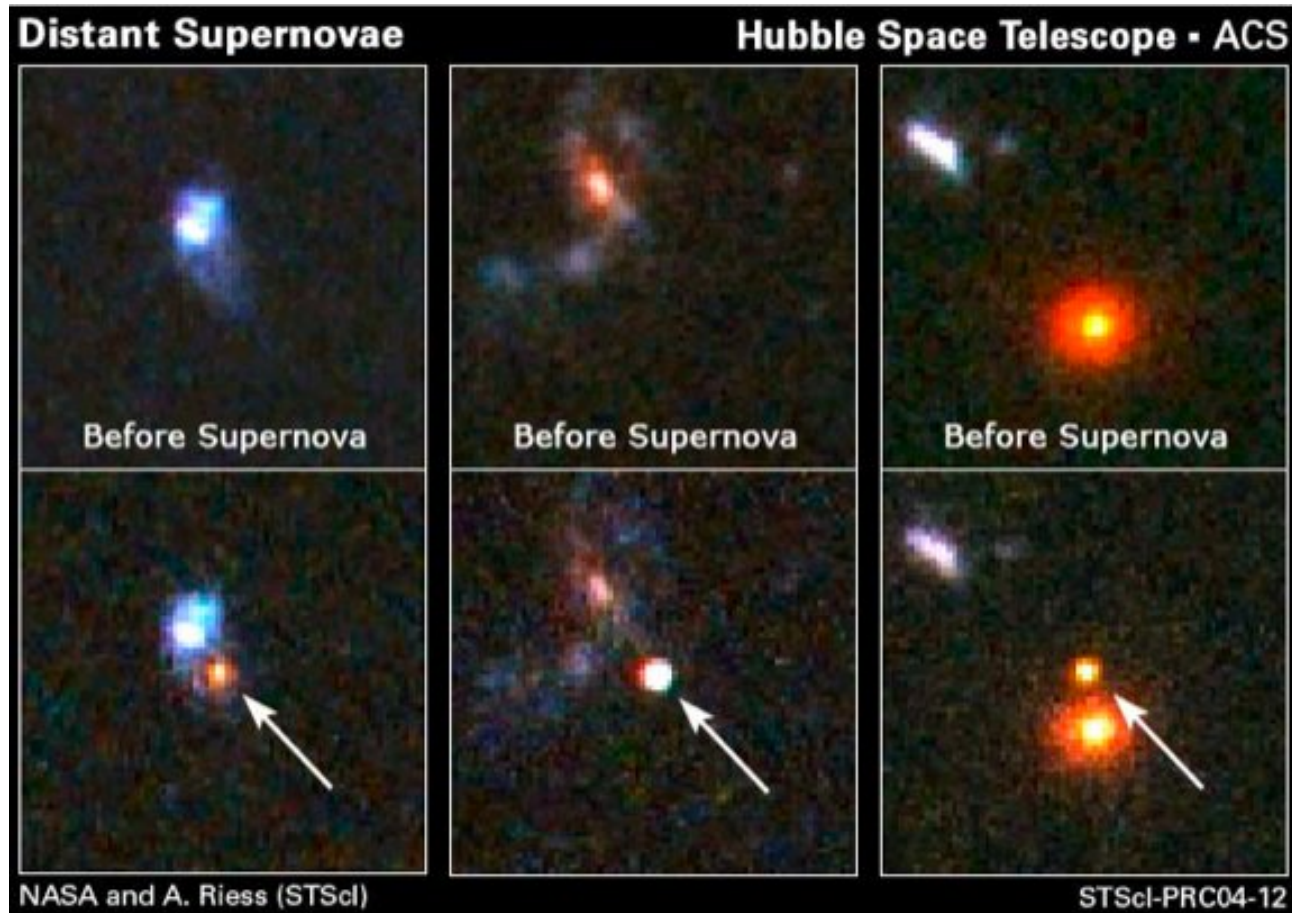
- Supernova Cosmology Project (<http://panisse.lbl.gov/>, P.I. Saul Perlmutter)
- High-z SN Search (<http://cfa-www.harvard.edu/supernova//HighZ.html>, P.I. Brian Schmidt)



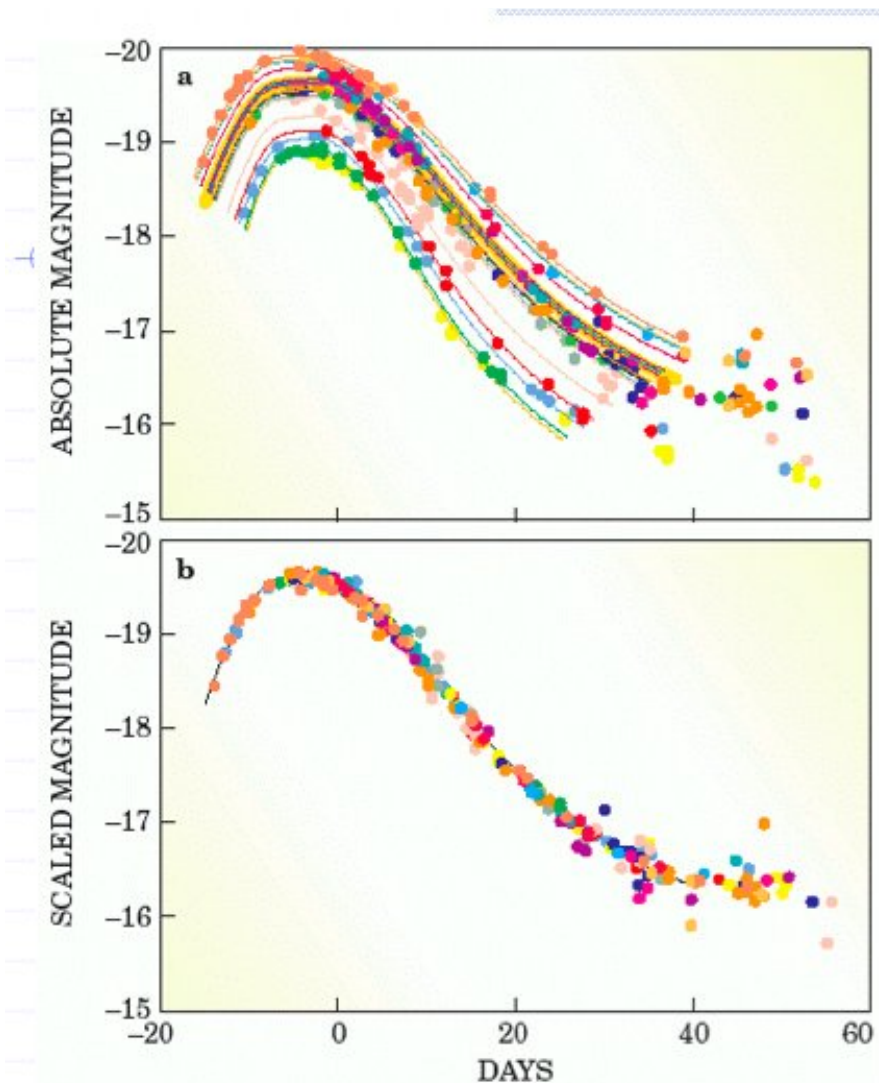
Secondary Indicators: high-z SNe (~4Gpc)

Two teams doing high-z SN searches to measure cosmological parameters:

- Supernova Cosmology Project (<http://panisse.lbl.gov/>, P.I. Saul Perlmutter)
- High-z SN Search (<http://cfa-www.harvard.edu/supernova//HighZ.html>, P.I. Brian Schmidt)



Secondary Indicators: high-z SNe (\sim 4Gpc)

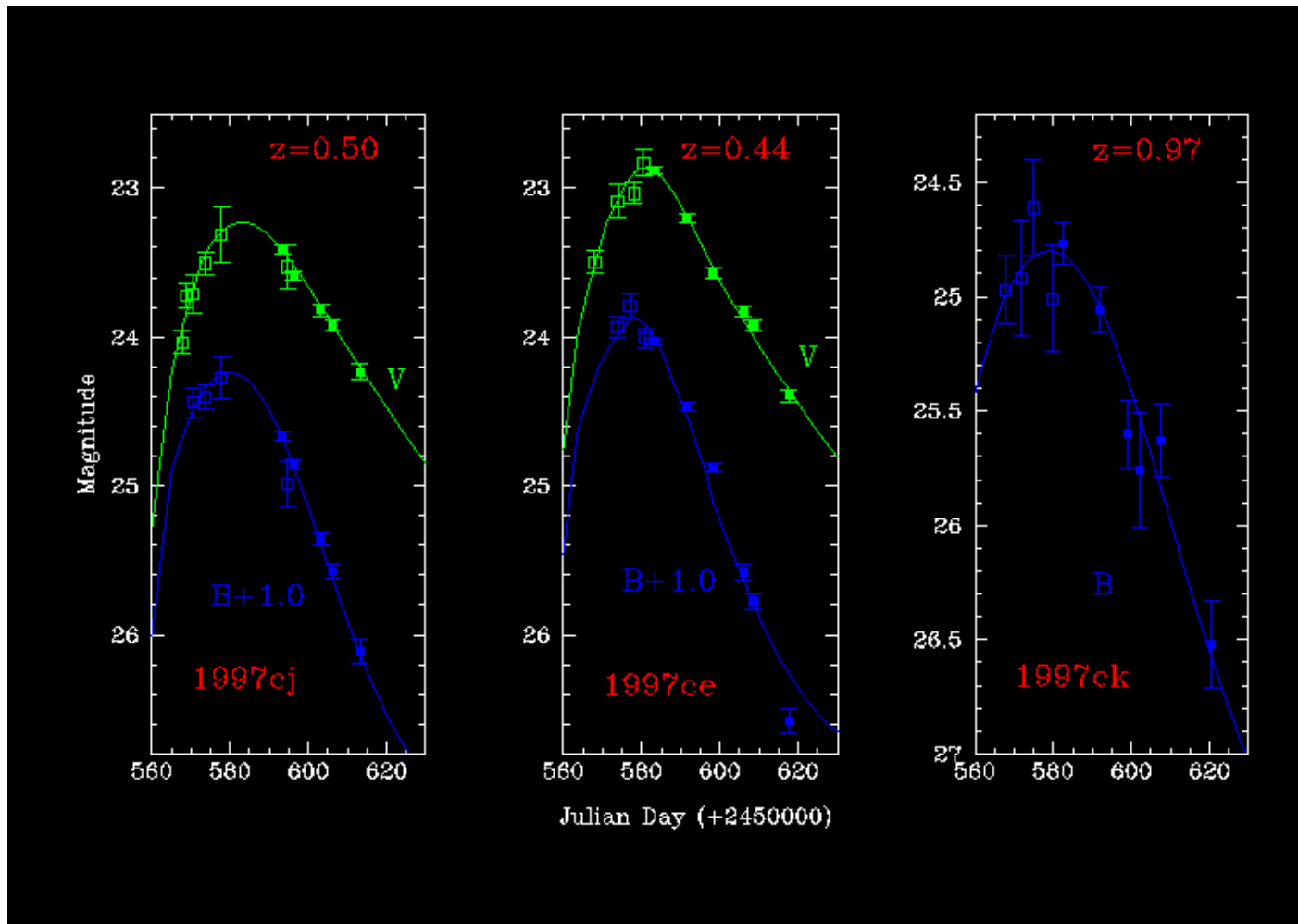


New methods to relate shape and luminosity and standardize luminosity at maximum:

SN Cosmo Project:
Stretch method
(Perlmutter et al. 1997)
High-z SN project:
Multi-colour light-shape fitting method
(Riess et al. 1996)

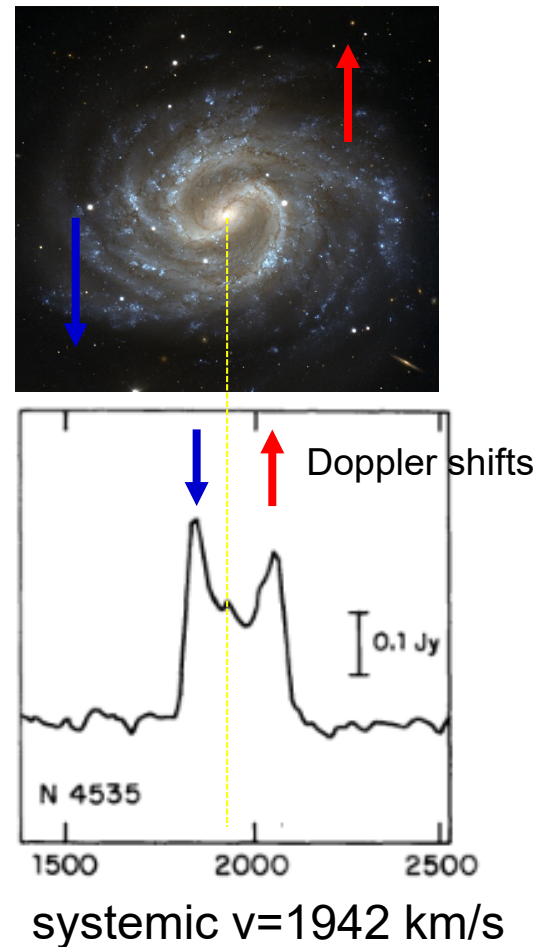
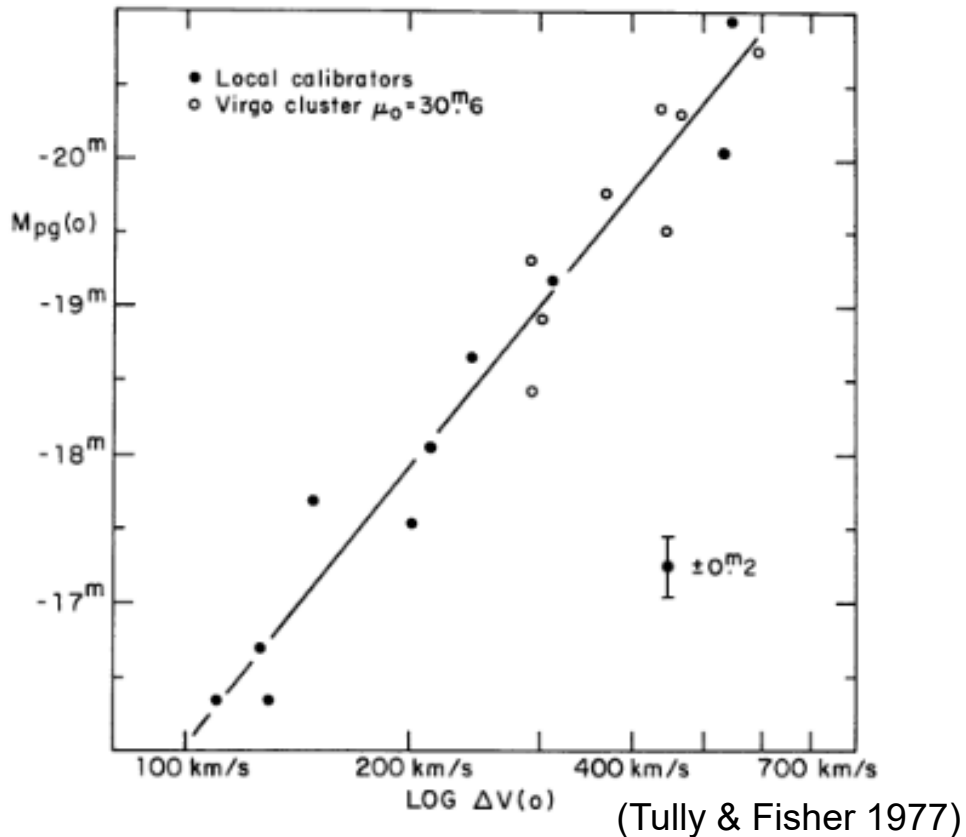
Secondary Indicators: high-z SNe (\sim 4Gpc)

Examples of light-curves by High-z SN Search Project (Garnavich et al. 1995)



Scaling relationships for Spirals: Tully-Fisher

Originally proposed (Tully & Fisher 1977) as a Distance Indicator, it is still used for this purpose, but it gives an understanding of the inner workings of S galaxies: **the maximal rotational velocity of S galaxies is related to the galaxy luminosity**, or in other words, it relates how fast they are rotating (DM halos) to their luminosities (baryons). Velocities originally derived from H₁ 21cm line profiles.



Scaling relationships for Spirals: Tully-Fisher

Why does it work?

In order to maintain the galaxy bound, using Newtonian mechanics

$$v_c = \sqrt{\frac{GM}{R}} \rightarrow M \propto R v_c^2$$

If we assume that the Surface brightness (i. e. luminosity per unit area) of all S galaxies is the same

$$SB \propto \frac{L}{R^2} \rightarrow L \propto R^2 \rightarrow R \propto L^{1/2}$$

Since the mass-to-light ratio can be expressed as $M = L(\frac{M}{L})$, and if M/L is approximately the same for all S galaxies, we can rewrite the 1st expression as

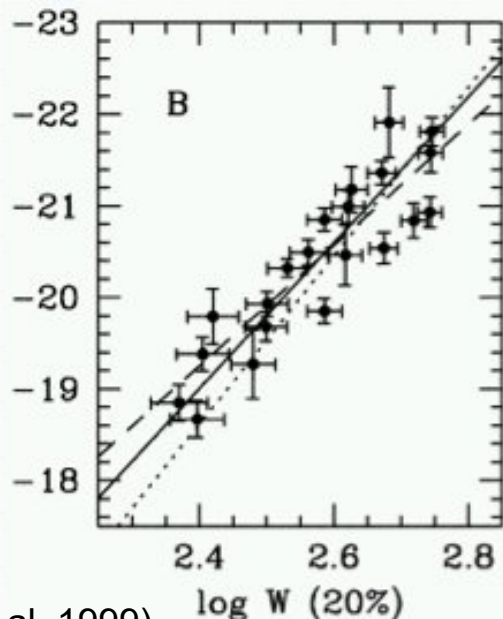
$$L\left(\frac{M}{L}\right) \propto L^{\frac{1}{2}} v_c^2 \rightarrow L^{\frac{1}{2}} \propto v_c^2 \rightarrow L \propto v_c^4.$$

Since $M = -2.5 \log(L) + \text{cte}$, in magnitudes we have

$$M \propto 10 \log v_c$$

And hence, if we measure the rotational velocity of a galaxy, we can infer its luminosity and mass, and hence we have a standarized candel to measure distances.

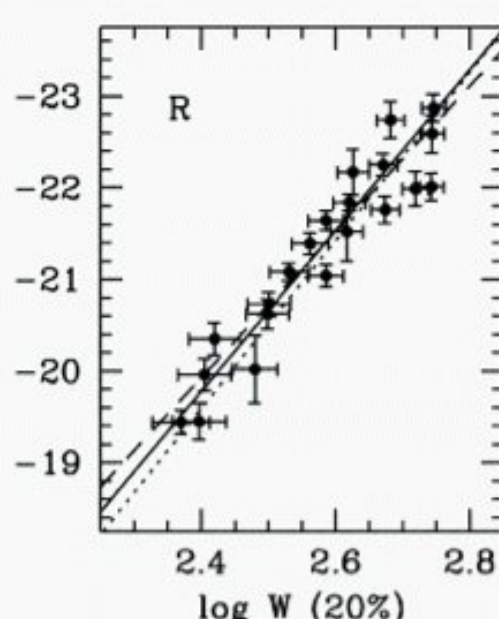
Scaling relationships for Spirals: Tully-Fisher



(Sakai et al. 1999)

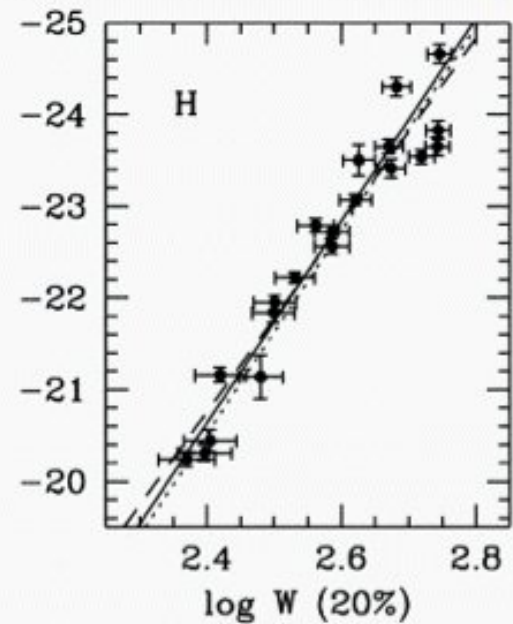
$$\alpha = 3.2$$

Scatter=0.25 mag



$$\alpha = 3.5$$

Scatter=0.25 mag



$$\alpha = 4.4$$

Scatter=0.19 mag

The relationship is not exactly $L \propto v_c^4$. It varies from band to band showing less scatter at IR wavelengths due to less importance of extinction corrections, and it also changes for different types of Spirals, for instance (Rubin 1978):

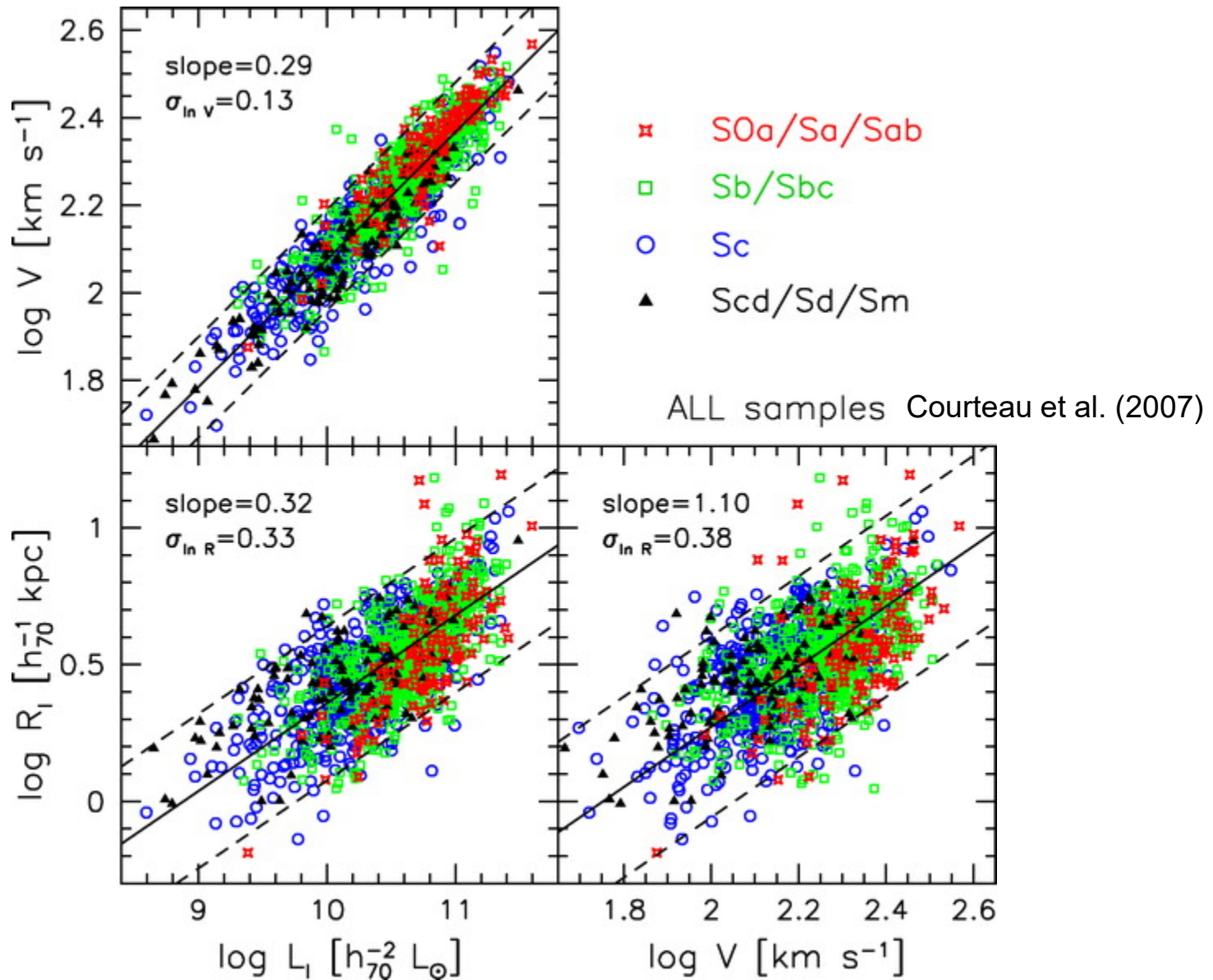
Notice that extinction is also correlated with Hubble type.

$$M_B = -9.95 \log v_{\max} + 3.15 \quad Sa$$

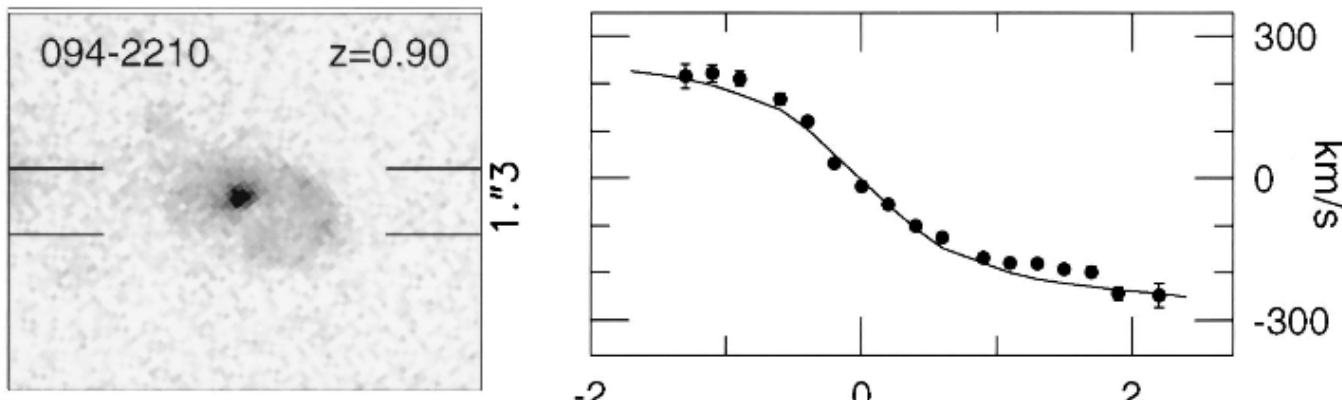
$$M_B = -10.2 \log v_{\max} + 2.71 \quad Sb$$

$$M_B = -11.0 \log v_{\max} + 3.31 \quad Sc$$

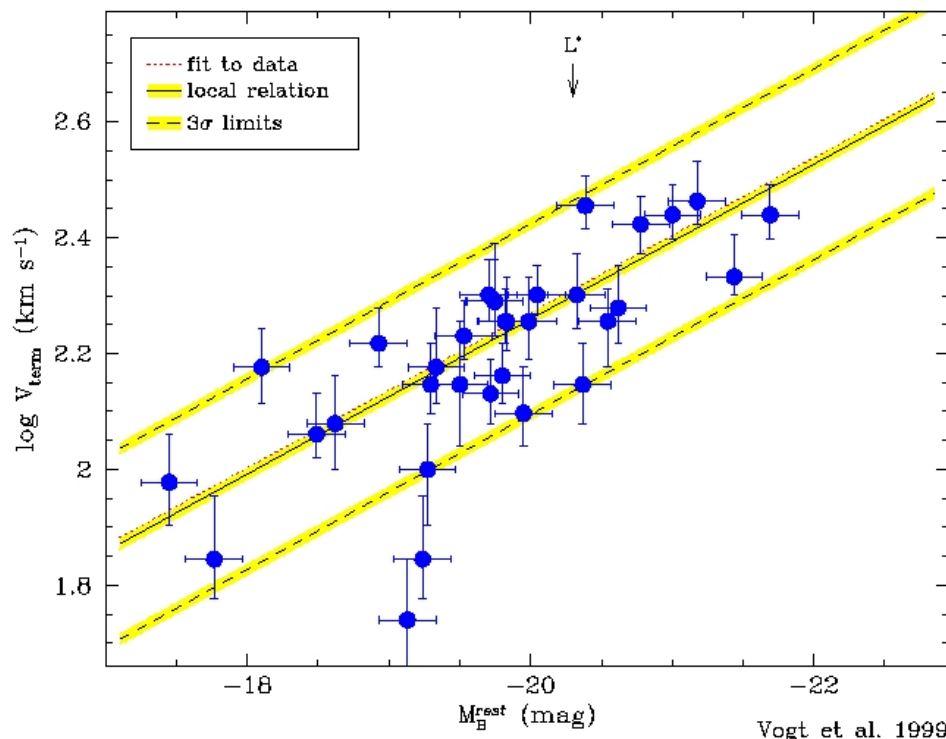
Scaling relationships for Spirals: Tully-Fisher



Scaling relationships for Spirals: Tully-Fisher at high-z



TULLY-FISHER RELATION TO $z \sim 1$

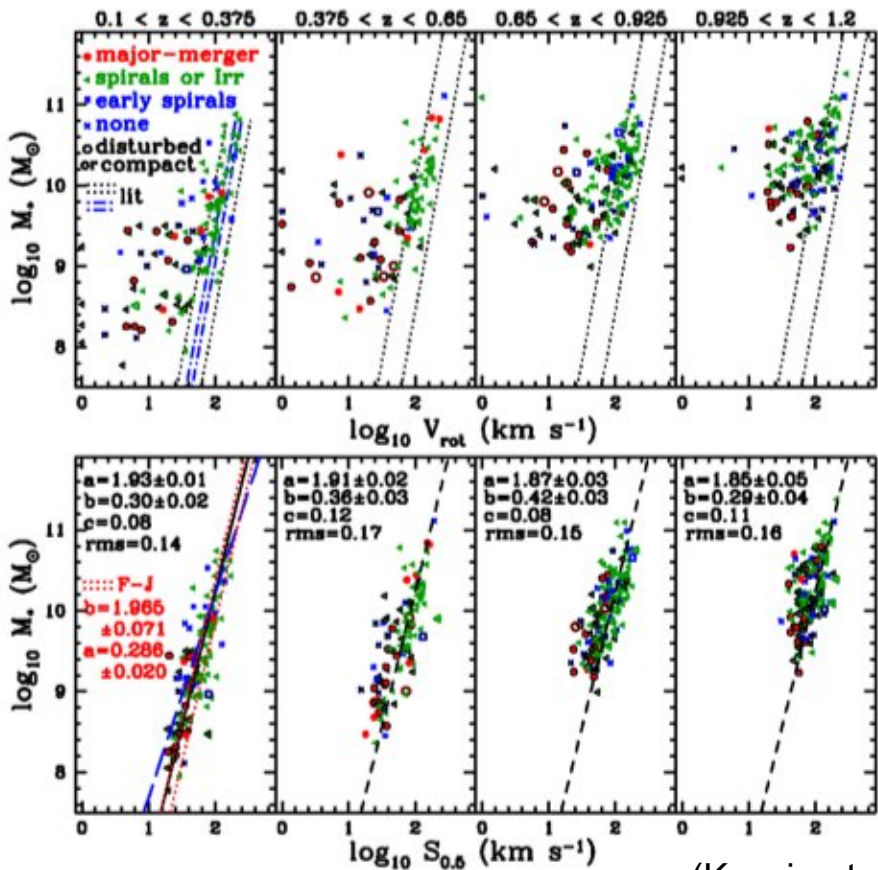


(Vogt et al. 1996, 1999)

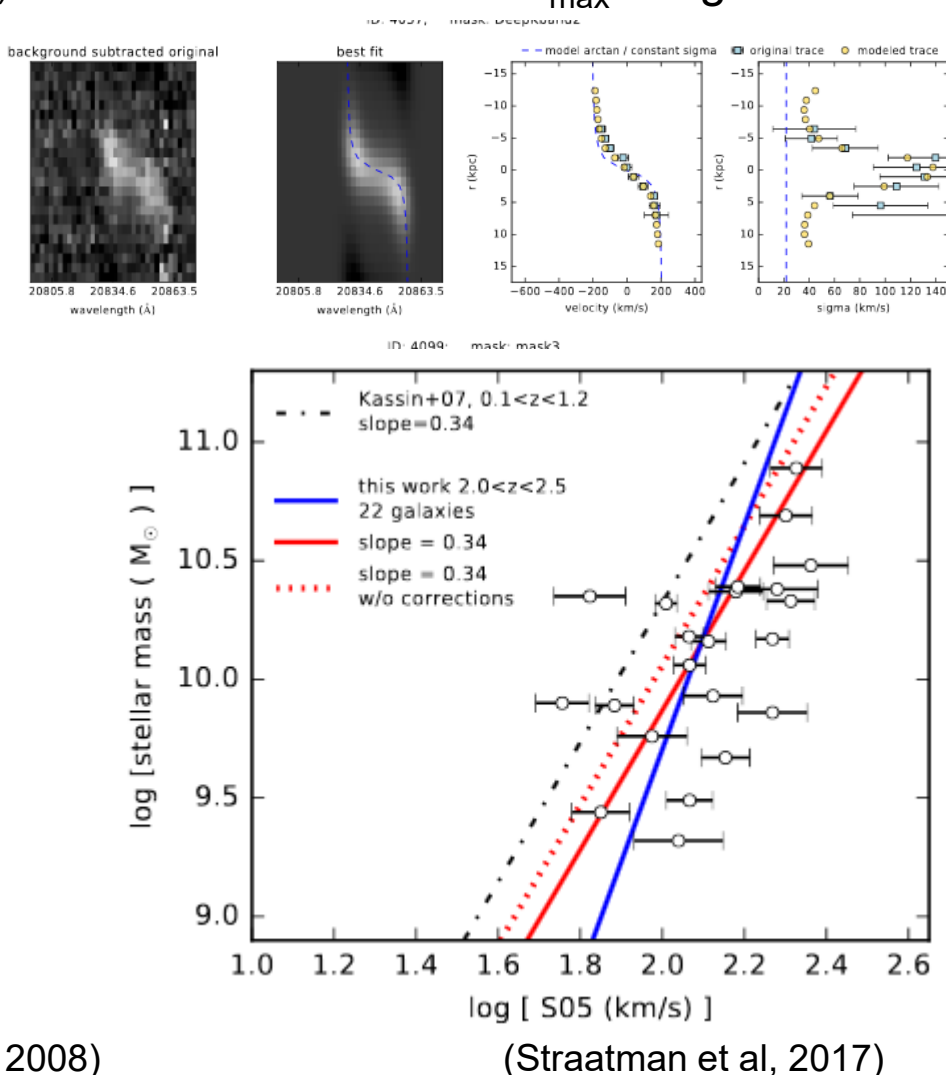
The relationship can be traced to galaxies at $z \sim 1$ (when the age of the Universe was only 5.9Gyr). Velocities measured from H α and [O II] 3727Å emission lines in the spectrum along the slit.

Scaling relationships for Spirals: Tully-Fisher at $z < 2.5$

It is nowadays expressed as a function of stellar mass or gas+stellar mass. At $z \sim 2$ evolution starts to be inferred: $\Delta M/M_{\odot} = -0.45 \pm 0.13$ dex compared to $z \sim 1$. A modified velocity $S_{0.5} = \sqrt{0.5v_{rot}^2 + \sigma_{gas}^2}$ (Kassin et al. 2008) is introduced instead of v_{max} to tighten the relationship.



(Kassin et al 2008)



(Straatman et al, 2017)

Secondary Indicators: D_n - σ (~ 1 Gpc)

E galaxies have a **fundamental plane** that links their surface brightness, luminosity and velocity dispersion: $L \propto I_0^x \sigma^y$ with $x \sim -0.7$, $y \sim 0.3$ (Dressler et al. 1987, Djorgovski & Davis 1987).

This relationship can be understood if E gal are self-gravitating systems with roughly constant M/L ratios.

$$\text{Virial Theorem } \sigma^2 \propto M/r_0$$

$$M/L \propto M^a$$



$$L^{1+a} \propto \sigma^{4-4a} I_0^{a-1}$$

$$\text{de Vaucouleurs profile} \Rightarrow L \propto I_0 r_0^2$$

If we measure the diameter of an E gal within which the mean surface brightness takes some reference value $D_n \propto r_0^\alpha I_0^\beta$ and we choose that reference level such that $\sigma \propto D_n^\delta$

$$\log D_n = 1.3 \log \sigma + C$$

where $C = C(d)$

The reference brightness level is 20.75 mag/arcsec² in B.

Good for relative distances and usually applied to clusters (e.g. Virgo-Coma)

Secondary Indicators: D_n - σ (~ 1 Gpc)

D_n - σ Relation

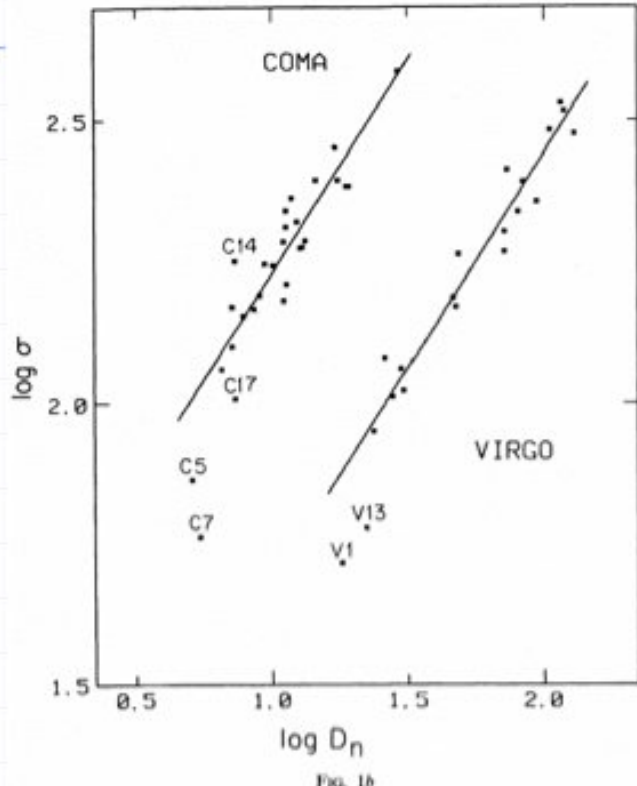


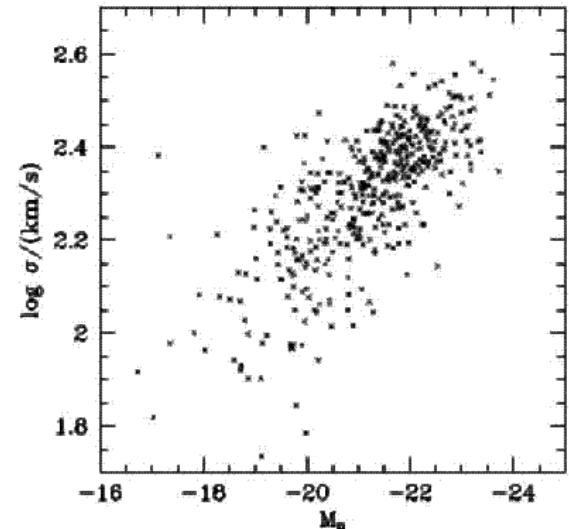
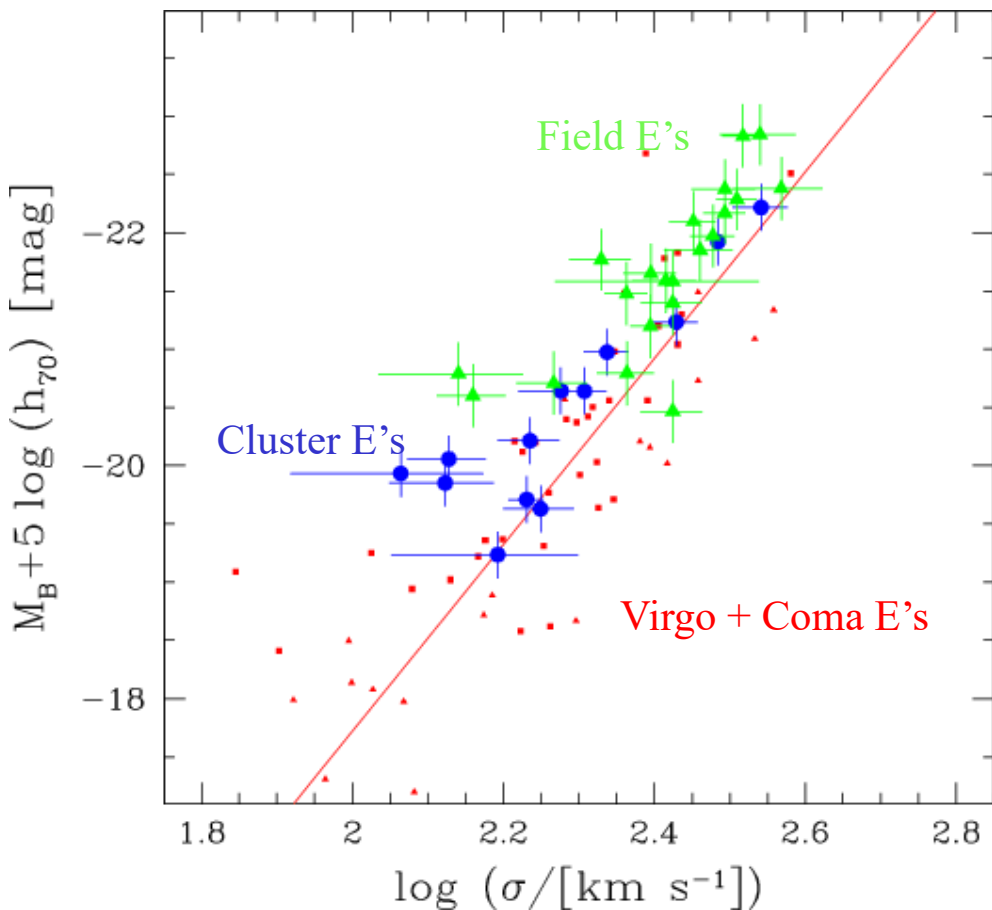
FIG. 1.—(a) B_T , the total blue magnitude, vs. $\log \sigma$, the central velocity dispersion, for ellipticals in the Coma and Virgo clusters. These are the variables of the Faber-Jackson relationship. The lines $\log \sigma = -0.114B_T + C$, where $C = 3.561$ for Virgo and $C = 3.960$ for Coma, are best median fits, as described in the text. The rms scatters in B_T from these lines are 0.57 mag for Virgo and 0.69 mag for Coma. (b) $\log D_n$, the diameter within which the integrated blue surface brightness is $20.75 B$ mag arcsec $^{-2}$, vs. $\log \sigma$ for the same galaxies. The horizontal scales correspond to a factor of 10 in distance in both figures. The lines $\log \sigma = 0.750 \log D_n + C$, where $C = 0.934$ for Virgo and $C = 1.475$ for Coma, are best median fits. The rms scatter in $\log D_n$ is 0.059 for Virgo and 0.072 for Coma, a factor of 2 smaller scatter than with the Faber-Jackson relationship.

From Dressler et al (1987) the offset gives the relative Distance, but note the scatter!

Secondary Indicators: Faber-Jackson ($\sim 1\text{Gpc}$)

In the absence of surface-brightness information, still the relationship holds
(Faber & Jackson 1976):

$$L \propto \sigma^\alpha \text{ with } \alpha \approx 3-4$$

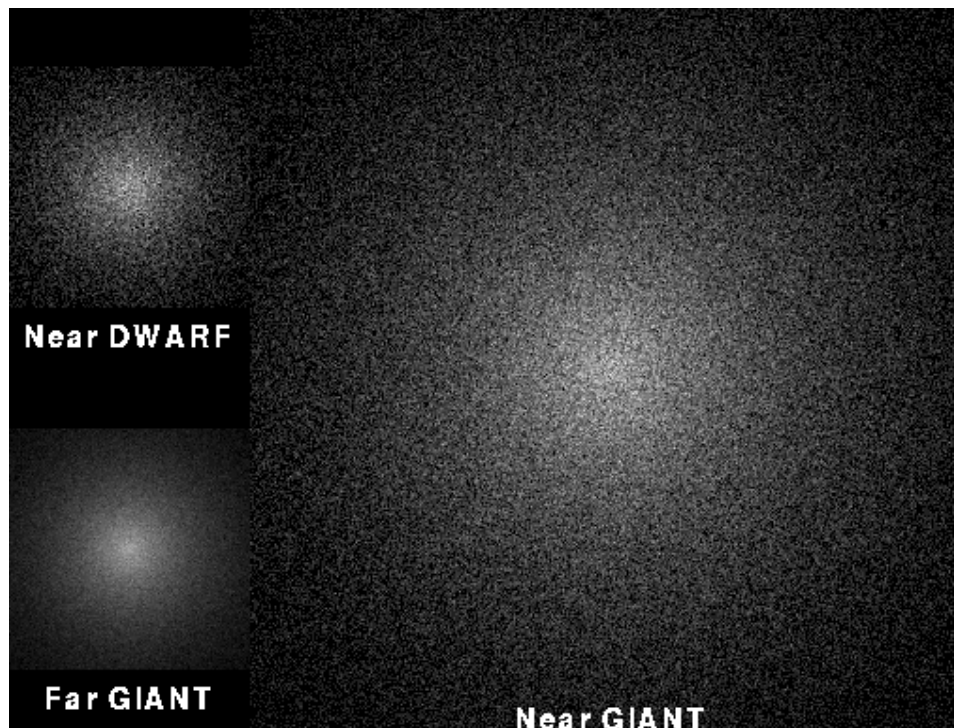


Modest B-evolution of 0.3-0.5mag
at $z \sim 0.4-0.7$
(e.g. Ziegler et al. 2005)

Other Secondary Indicators: Surface Brightness Fluctuations

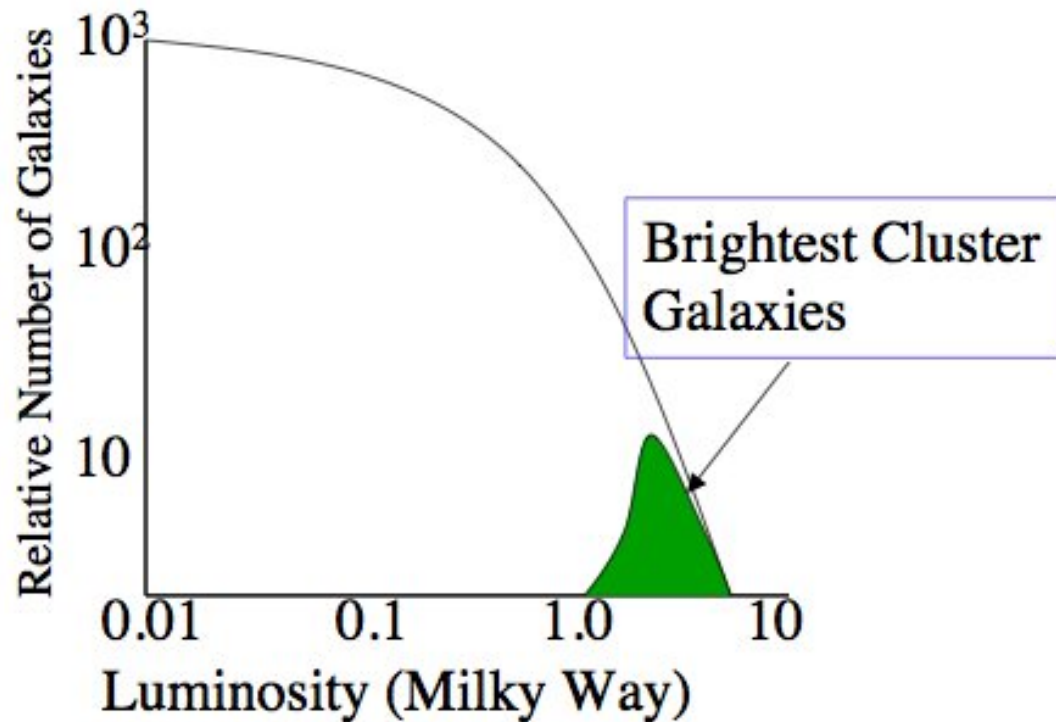
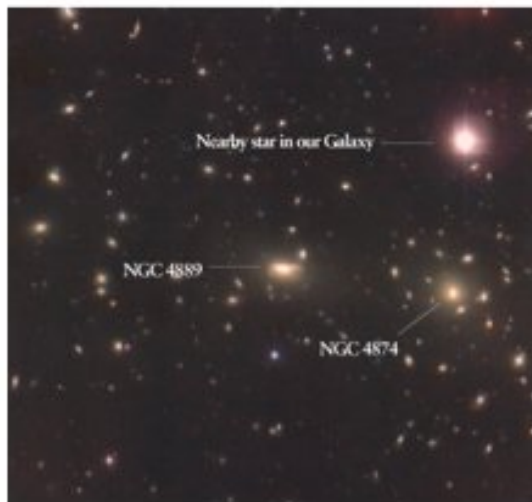
Statistical fluctuation in the number of stars in a pixel (Tonry & Schneider 1988, Tonry et al. 2000)

A nearby galaxy: $100/\text{pixel} \pm 10\%$ fluctuations
A distant galaxy: $1000/\text{pixel} \pm 3\%$ fluctuations



Other Secondary Indicators:

Brightest Galaxy in Cluster



Note the narrow range in luminosity - thus standard candle.

Problem: rich clusters will have bright galaxies, but poor ones probably not

TABLE 1
NUMBERS OF CEPHEID CALIBRATORS FOR SECONDARY METHODS

Secondary Method	σ (%)	N (pre- <i>HST</i>)	σ_{mean} (%)	N (post- <i>HST</i>)	σ_{mean} (%)
Tully-Fisher relation	$\pm 20^{\text{a}}$	5 ^b	± 10	21	± 5
Type Ia supernovae	$\pm 8^{\text{c}}$	0	n/a	6 ^d	± 4
Surface brightness fluctuations.....	$\pm 9^{\text{e}}$	1	± 9	6	± 4
Fundamental plane.....	± 14	0	n/a	3 ^f	± 10
Type II supernovae	$\pm 12^{\text{g}}$	1	± 12	4	± 6

^a Giovanelli et al. 1997.

^b M31, M33, NGC 2403, M81, NGC 300; Freedman 1990.

^c Hamuy et al. 1996.

^d Using the distances to the host galaxies to SN 1937C, 1972E, 1981B, 1989B, 1990N, and 1998bu, but excluding 1895B, 1960F, 1974G.

^e Tonry et al. 1997.

^f Calibration based on Cepheid distances to Leo I group, Virgo and Fornax Clusters.

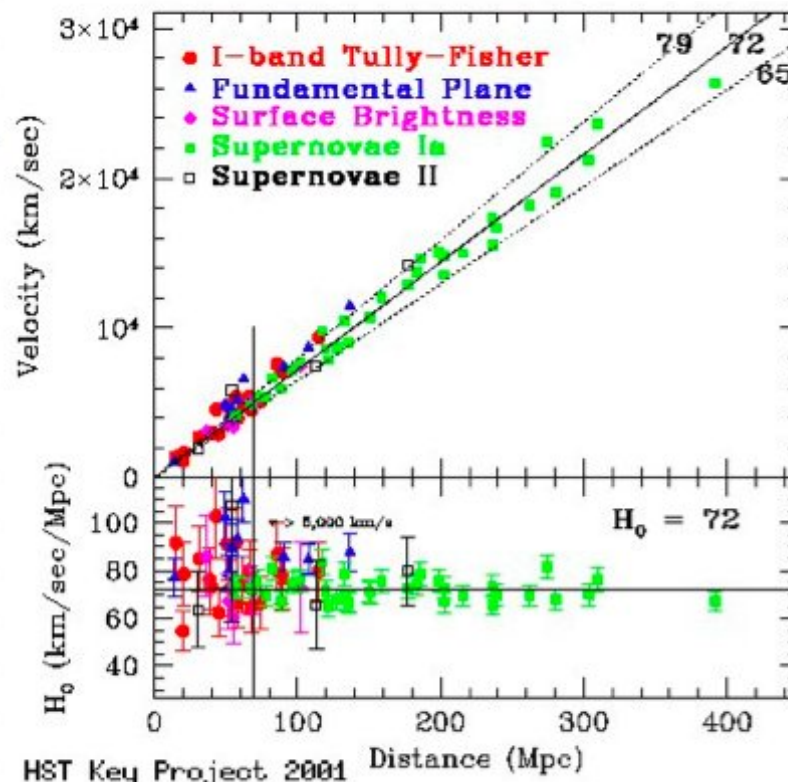
^g This paper; Schmidt et al. 1994 distant clusters.

(H_0 Key Project, Freedman et al. 2001)

The value of H_0 :

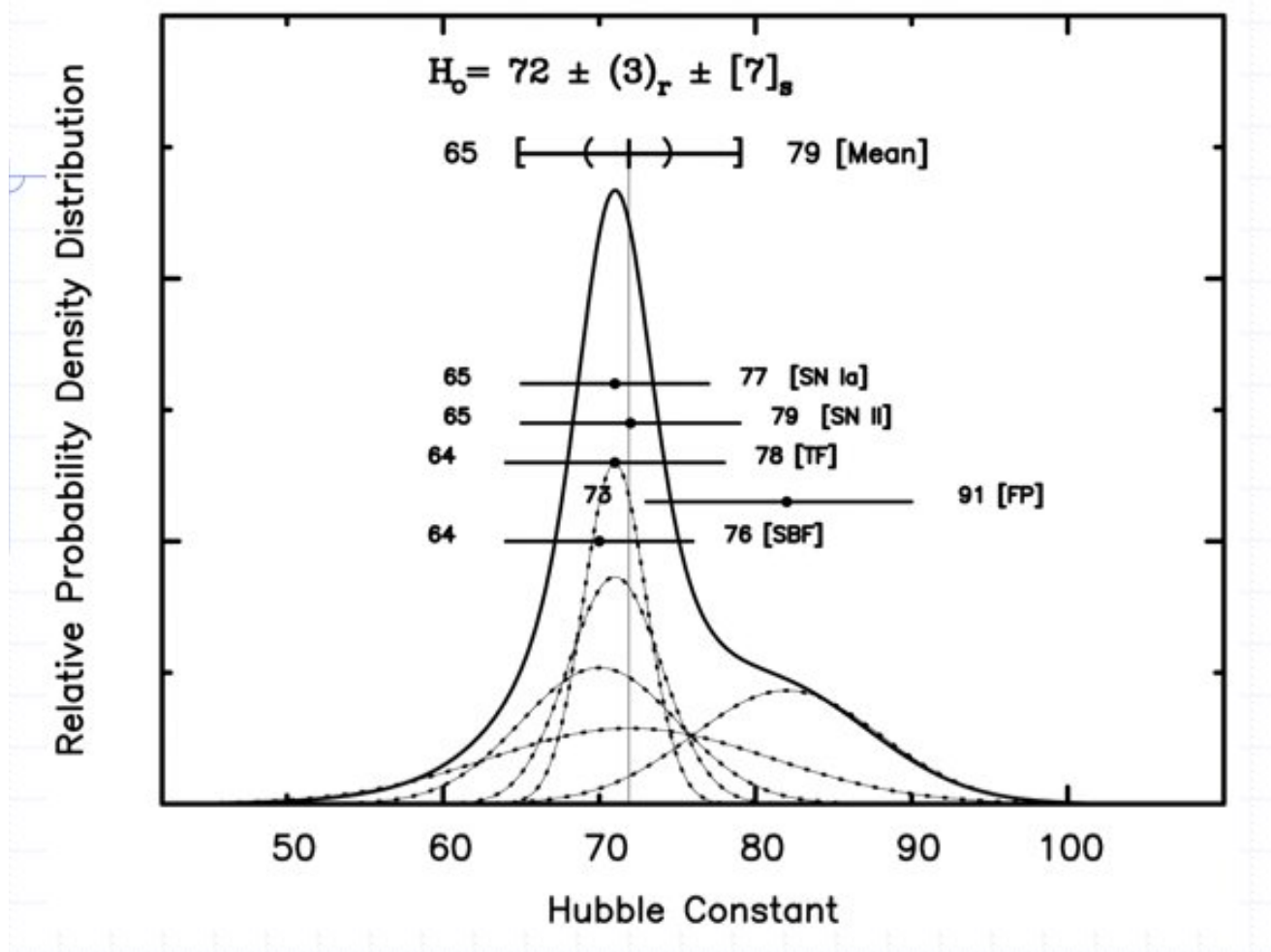
$$H_0 = 72 \pm 8 \text{ km/s/Mpc} \text{ (Freedman et al. 2001)}$$

(...) Based on these revised Cepheid distances, we find values (in $\text{km s}^{-1} \text{ Mpc}^{-1}$) of $H_0 = 71 \pm 2$ (random) ± 6 (systematic) (Type Ia supernovae), $H_0 = 71 \pm 3 \pm 7$ (Tully-Fisher relation), $H_0 = 70 \pm 5 \pm 6$ (surface brightness fluctuations), $H_0 = 72 \pm 9 \pm 7$ (Type II supernovae), and $H_0 = 82 \pm 6 \pm 9$ (fundamental plane). We combine these results for the different methods with three different weighting schemes, and find good agreement and consistency with $H_0 = 72 \pm 8 \text{ km s}^{-1} \text{ Mpc}^{-1}$ (...)



The value of H_0 :

$H_0 = 72 \pm 8 \text{ km/s/Mpc}$ (Freedman et al. 2001)



The value of H_0 :

$H_0 = 72 \pm 8$ km/s/Mpc (Freedman et al. 2001)

TABLE 14
OVERALL SYSTEMATIC ERRORS AFFECTING ALL METHODS

Source of Uncertainty	Description	Error (%)
LMC zero point	Error on mean from Cepheids, TRGB, SN 1987A, red clump, eclipsing binaries	± 5
WFPC2 zero point	Tie-in to Galactic star clusters	± 3.5
Reddening	Limits from NICMOS photometry	± 1
Metallicity	Optical, NICMOS, theoretical constraints	± 4
Bias in Cepheid PL	Short-end period cutoff	± 1
Crowding	Artificial star experiments	$+5, -0$
Bulk flows on scales $> 10,000$ km s $^{-1}$	Limits from SN Ia, CMB	± 5

NOTE.—Adopted final value of H_0 : $H_0 = 72 \pm 3$ (random) ± 7 (systematic) km s $^{-1}$ Mpc $^{-1}$.

The value of H_0 :

$H_0 = 72 \pm 8$ km/s/Mpc (Freedman et al. 2001)

TABLE 13
LMC DISTANCE MODULI FOR DIFFERENT METHODS

Method	$\langle \mu_0 \rangle^a$ (mag)	σ (mag)	N	$\langle \mu_0 \rangle^b$ (mag)	σ (mag)	N
Cepheids	18.57	± 0.14	5	18.52	± 0.13	15
Eclipsing variables	18.33	± 0.05	3
SN 1987A	18.47	± 0.08	4	18.50	± 0.12	5
TRGB	18.64	± 0.05	2	18.42	± 0.15	1
Red clump	18.27	± 0.11	10
RR Lyrae variables	18.30	± 0.13	7	18.40	± 0.19	14
Mira variables	18.54	± 0.04	3	18.46	± 0.11	4

^a Based on Gibson 2000 compilation.

^b Based on Westerlund 1997 compilation.

The value of H_0 :

LMC Distance modulus (Gibson 2000)

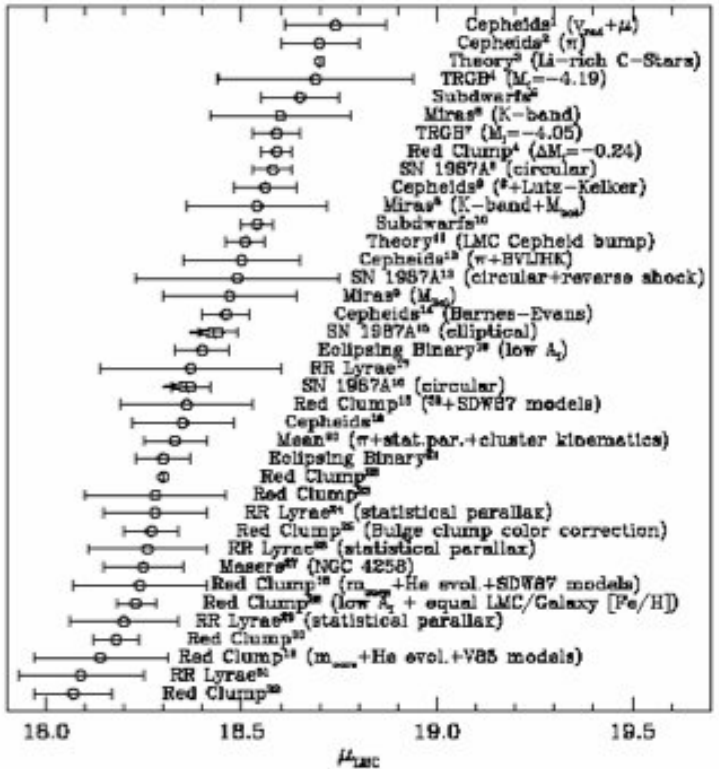


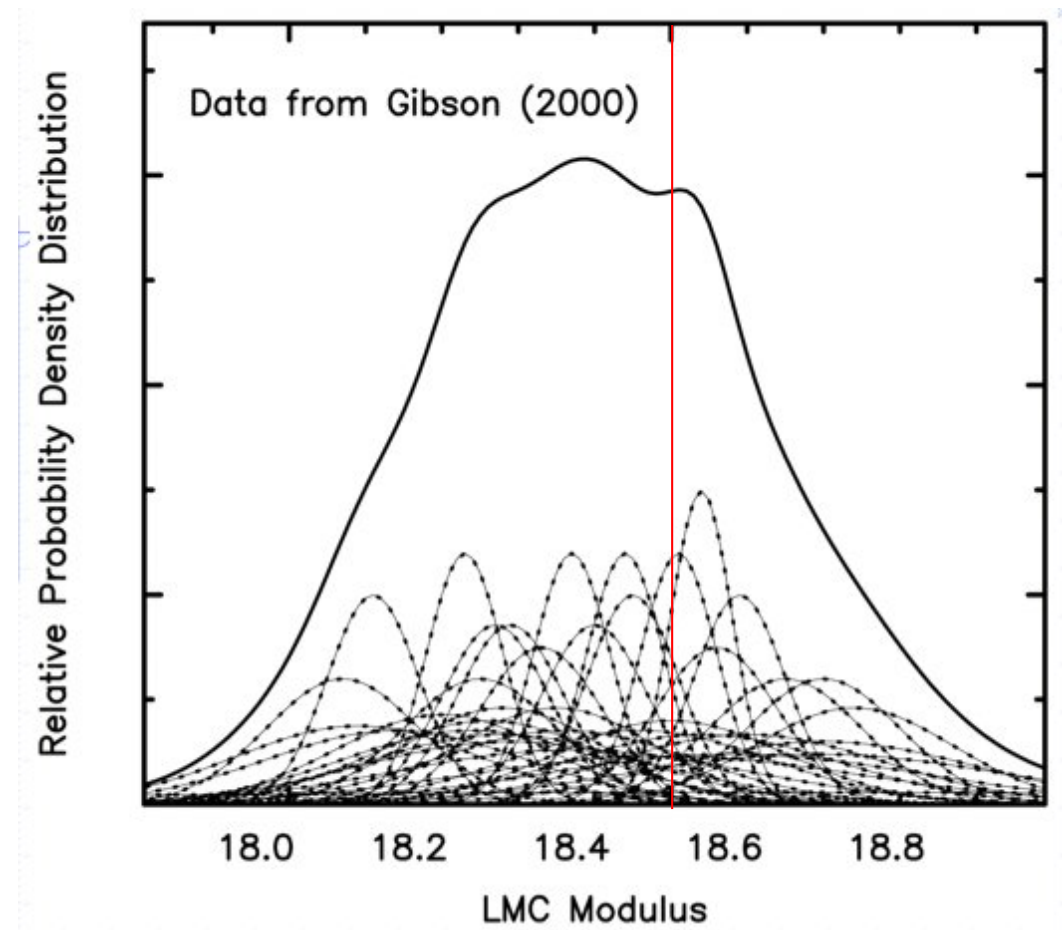
Fig. 1. Compilation of recent distance determinations to the LMC, presented in decreasing order of modulus μ_{LMC} . Cepheids, fitting to local Galactic subgiant sequences, and theoretical stellar models tend to favor the “long” distance scale (i.e., $\mu_{\text{LMC}} \gtrsim 18.5$, while RR Lyrae, red clump luminosities, eclipsing binaries, and masers (indirectly, through NGC 4258) tend to favor the “short” scale (i.e., $\mu_{\text{LMC}} \lesssim 18.4$). References: ¹Feast et al. (1998); ²Feast & Catchpole (1997); ³Ventura et al. (1999); ⁴Romaniello et al. (1999); ⁵Reid (1997); ⁶van Leeuwen et al. (1998); ⁷Sakai et al. (2000); ⁸Paragi (1998); ⁹Oudmaijer et al. (1998); ¹⁰Canetta et al. (1999); ¹¹Wood (1998); ¹²Madore & Freedman (1998); ¹³Garnavich et al. (1999); ¹⁴Gieren et al. (1998); ¹⁵Gould & Uza (1998); ¹⁶Nelson et al. (1999); ¹⁷Luri et al. (1998); ¹⁸Cole (1998); ¹⁹Luri et al. (1999); ²⁰Popowski & Gould (1999); ²¹Guinan et al. (1998); ²²Beaulieu & Sackett (1998); ²³Girardi et al. (1998); ²⁴Layden et al. (1996); ²⁵Fernley et al. (1998); ²⁶Popowski (1999); ²⁷Maoz et al. (1999); ²⁸Udalski (1999); ²⁹Popowski & Gould (1998) and Gould & Popowski (1998); ³⁰Udalski (1998b); ³¹Udalski (1998a); ³²Stanek et al. (1998).

The value of H_0 :

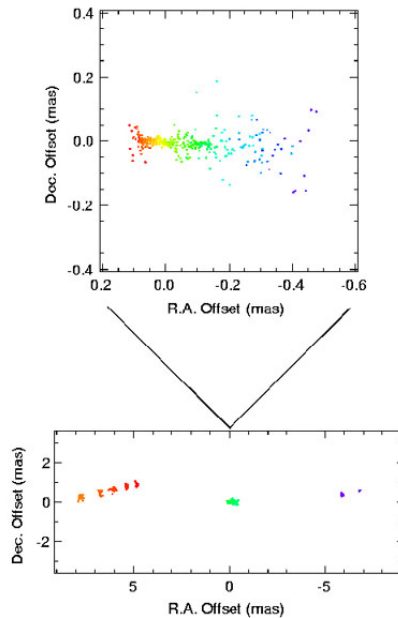
LMC Distance modulus (Gibson 2000)

Mean 18.45 ± 0.06

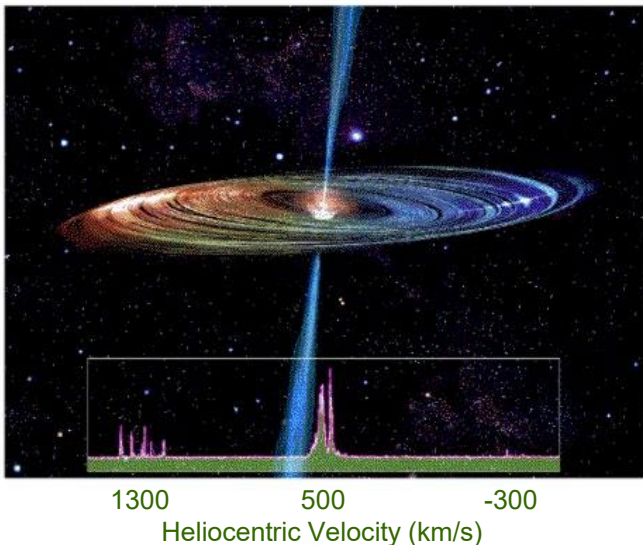
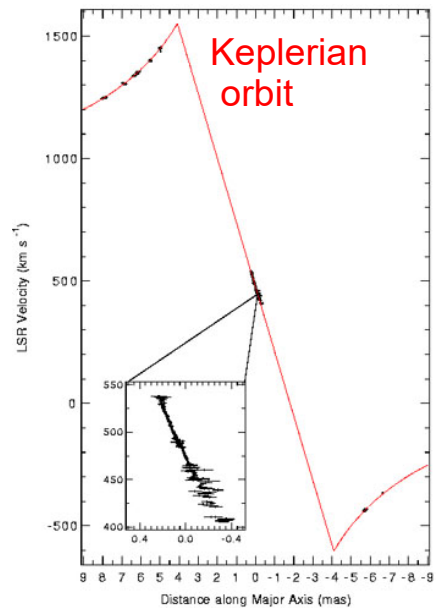
H_0 Key project assumes 18.5



Geometrical distance to NGC4258



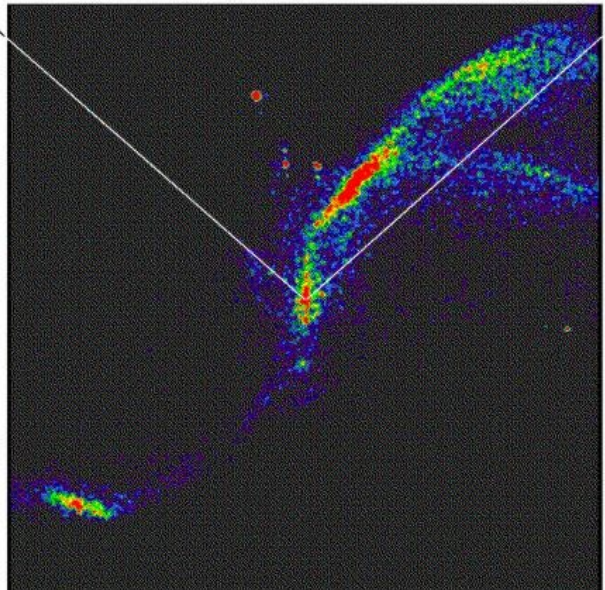
(Miyoshi et al. 1995)



NGC 4258

0.5 ly

1 cm



20 cm

10,000 ly

H_2O megamaser @ 22 GHz detected in a warped annulus of 0.14 – 0.28pc and less than 10^{15} cm of thickness, with a beaming angle of 11° (Miyoshi et al. 1995, Maloney 2002) has been used to measure the distance to the galaxy (Humphreys et al. 2013): combining the Doppler velocities and accelerations, and the angular separation of the masers ($a=v^2/r$) $7.60 \pm 0.17 \pm 0.15$ Mpc

The value of H_0 with LMC at 1%: 74.0 ± 1.4 km/s/Mpc

Anchor use LMC, MW and NGC4258 (Riess et al. 2019), including primary indicators such as detached eclipsing binaries that better calibrate the Cepheid zero-points

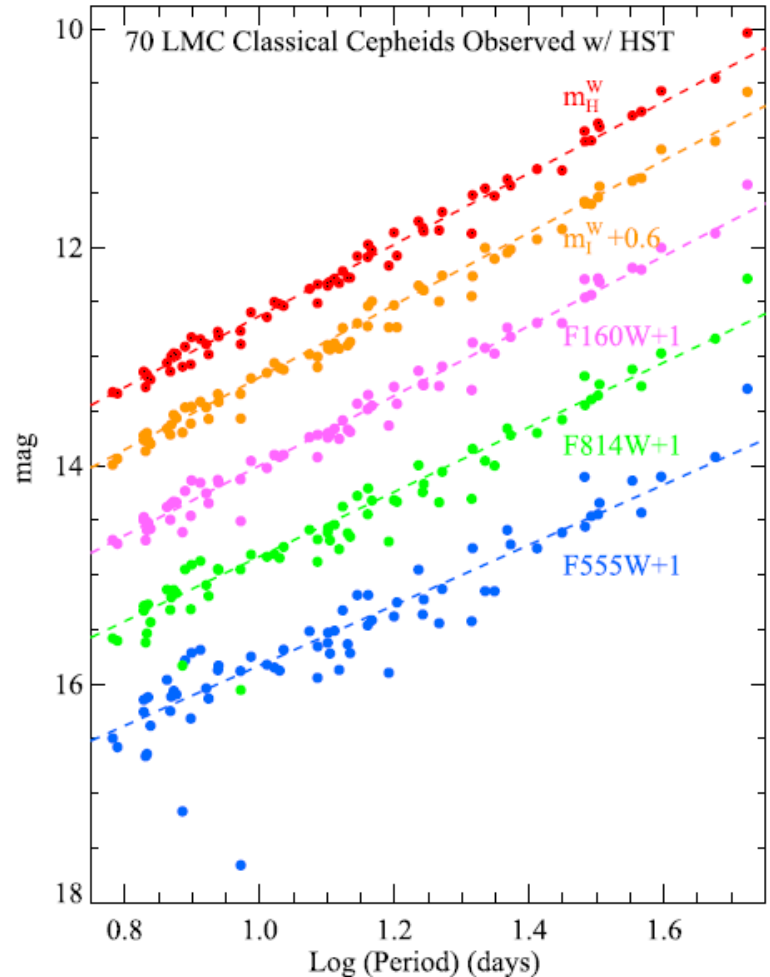


Figure 3. Period–mean magnitude relation for the 70 LMC Cepheids with slopes and statistics given in Table 3.

The value of H_0 :

Publications of the Astronomical Society of the Pacific
108: 1073–1082, 1996 December

H_0 : The Incredible Shrinking Constant 1925–1975

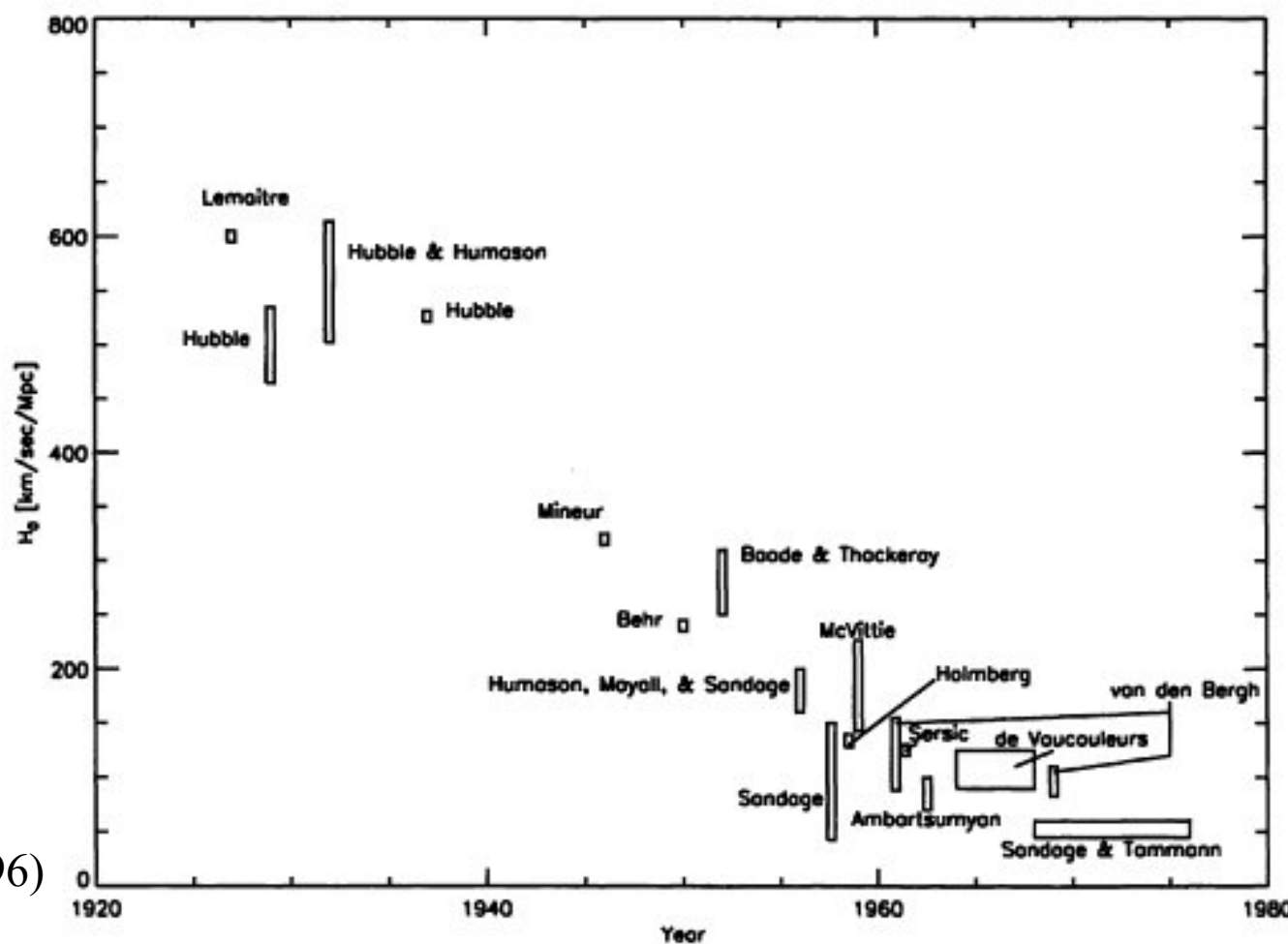
VIRGINIA TRIMBLE

Physics Department, University of California, Irvine, California 92717 and Astronomy Department, University of Maryland,
College Park, Maryland 20742

Received 1996 September 13; accepted 1996 September 30

ABSTRACT. The story of the Hubble constant logically begins just where the Curtis–Shapley debate on the distance scale of the universe ended, with Hubble's discovery of Cepheid variables in several nebulae that we now recognized as galaxies within the Local Group, which settled the issue of the existence of external galaxies. Hubble's own value of H was in the range of $500\text{--}550 \text{ km s}^{-1} \text{ Mpc}^{-1}$. The “best buy” value shrank in several large steps beginning in 1952, each being predicated on the recognition of some fundamental mistake in the previous distance scale calibrations. But it shrank more for some workers than for others, and by 1975 there was a clear polarization between a “long” and a “short” distance scale. On the theoretical side, important events were the recognition that general relativity permits, indeed nearly requires, an expanding universe; the gradual elimination of alternative explanations of redshift–distance relations; and the repelling of a late assault in the form of steady-state cosmology, within whose framework H_0 is a well-defined, never-varying number of only moderate importance.

The value of H_0 :

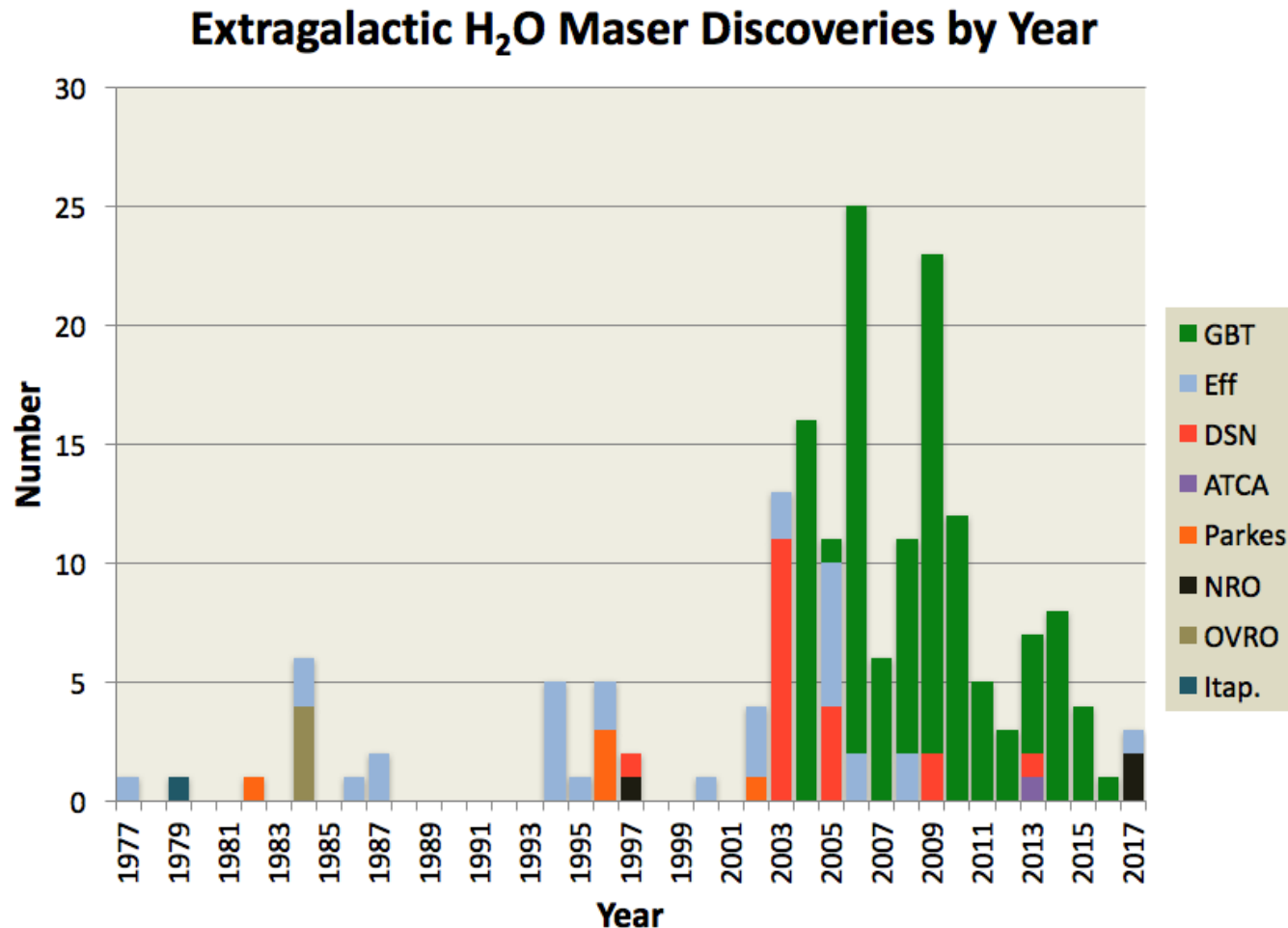


(Trimble 1996)

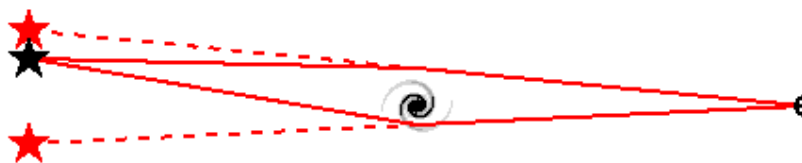
FIG. 1.—Published values of the Hubble constant from Lemaître (1927) to the hardening of the battle lines. Rectangle dimensions are intended to suggest a range of values/uncertainties or a range of dates. Except where the errors listed below are larger, all uncertainties were claimed to be of order 10% or less (occasionally much less). A straight-line fit to the numbers from 1927 to 1965 or so would have suggested that the Hubble constant might have become negative within a decade or two (discovered by astronomy graduate students at Caltech in the 1960s and undoubtedly by many others). This did not actually happen. The numerical values represented are Lemaître 600, Hubble 465, 513, 535; Hubble and Humason 526; Mineur 320; Behr 240; Baade and Thackeray 280±30; Hubble, Mayall, and Sandage 180±20; Sandage 75 (+75, -40); Holmberg 134±6; McVittie 143–227; Sersic 125±5; van den Bergh 100 (+20, -12), 120 (+25, -20); Ambartsumyan 70–100; de Vaucouleurs 125, 100±10, 100±10; van den Bergh 95 (+15, -12); Sandage and Tammann 45–60.

H0 without the distance ladder:

More Keplerian megamasers like NGC4258 (Pesce et al., 2020):
 73.9 ± 3.0 km/s/Mpc



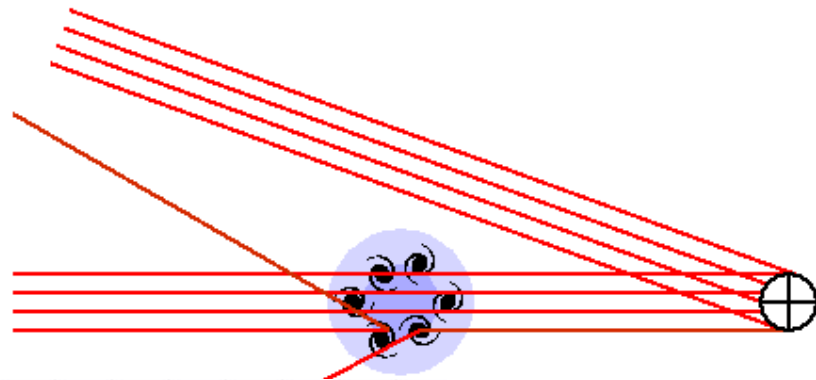
H0 without the distance ladder:



◆ Gravitational lens time delays

- Assuming the mass model for the lensing galaxy of a gravitationally lensed quasar is well-known (!?!)!, the different light paths taken by various images of the quasar will lead to time delays in the arrival time of the light to us. This can be traced by the quasar variability.
- This has been done for a handful of objects, find values of H0 between 50 and 70 km/s/Mpc ... lower on average than the Key Project values. (e.g. 0957+561 Kundic et al. 1997)
- If the lensing galaxy is in a cluster, we also need to know the mass distribution of the cluster and any other mass distribution along the line of sight. The modeling is complex!
- Because of this, gravitational lens time delay measurements depend on Ω_Λ and Ω_M .

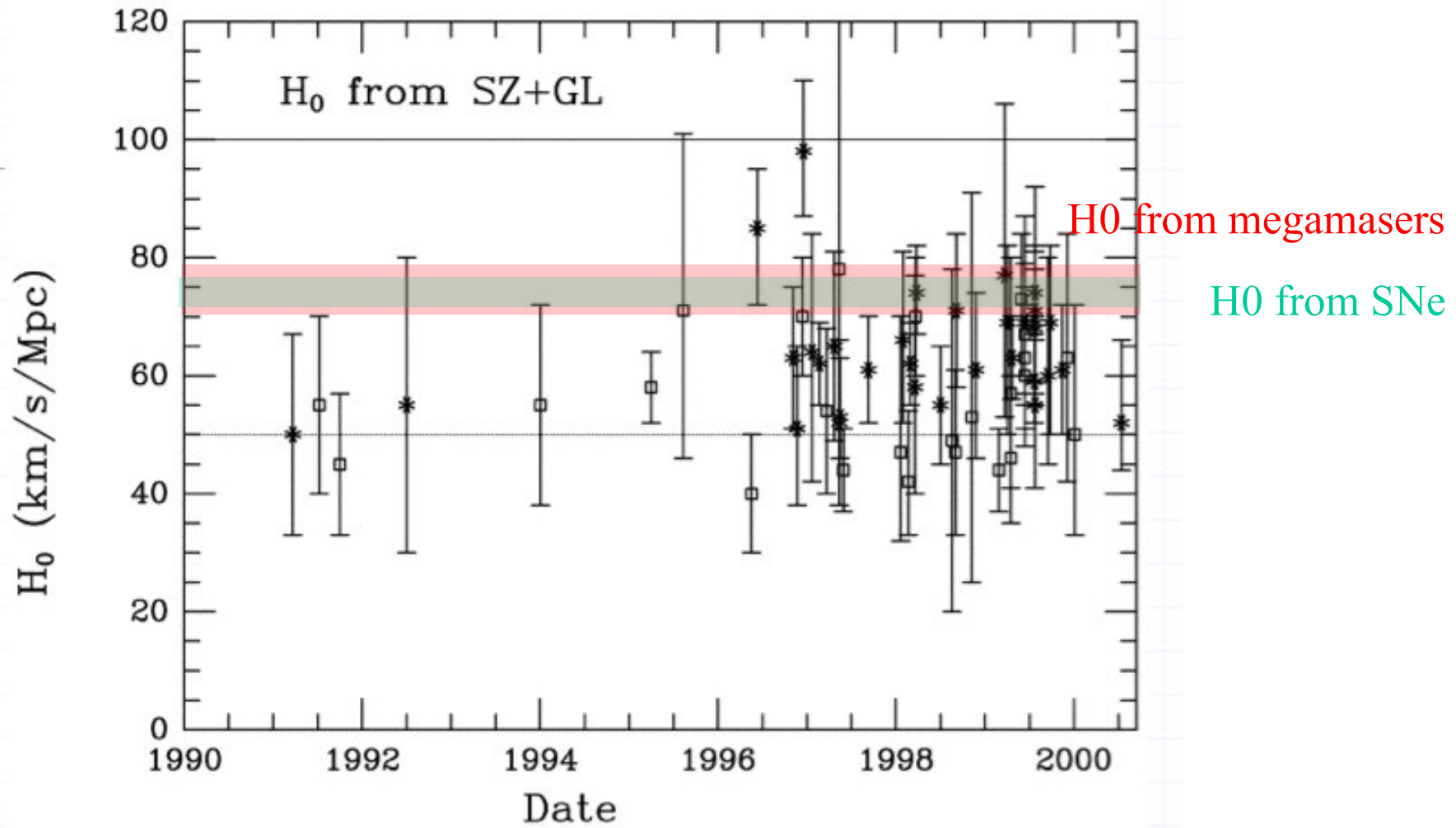
H₀ without the distance ladder:



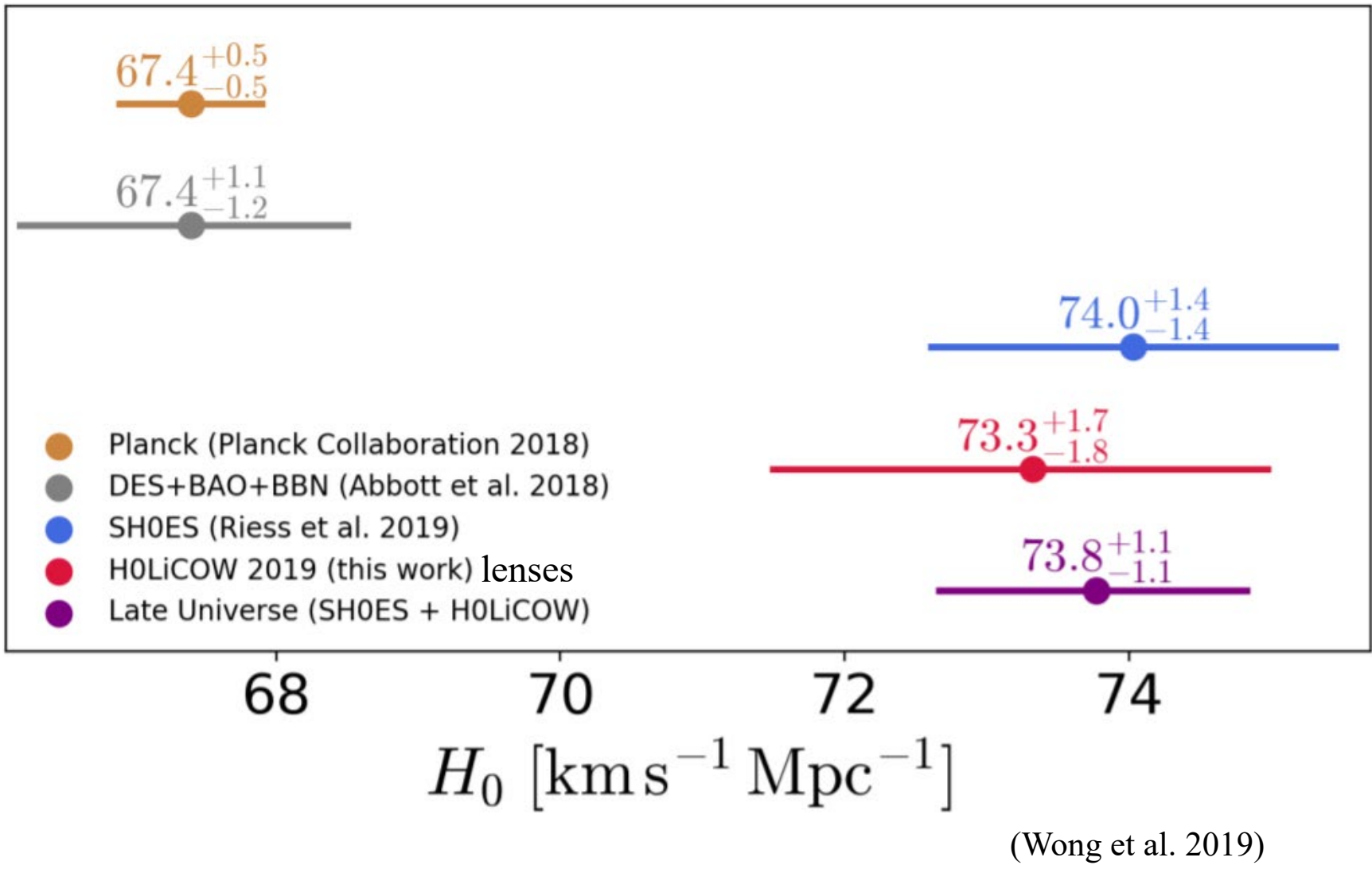
◆ The Sunyaev-Zel'dovich Effect

- The electrons in the intracluster medium will scatter the background photons from the cosmic microwave background (CMB) to higher energies (frequencies) and distort the blackbody spectrum
- If we can measure the electron density and temperature of the ICM along the line of sight from x-ray measurements and we assume the cluster is spherical (??) we can determine the distance to the cluster from the shift in the CMB spectrum
- Published values for H₀ range from 40 – 80 km/s/Mpc, most recent is H₀ = 60 +/- 10 km/s, but there are large systematic uncertainties (e.g. 38 clusters Bonamonte et al. 2006)
- Potential uncertainties include cluster substructure or shape (prolate instead of spherical). It's non-trivial to measure the x-ray temperature to derive the density at high redshifts.
- Need larger surveys for S-Z clusters at higher redshifts, these are underway!

H₀ without the distance ladder



flat Λ CDM



The original Hubble diagram

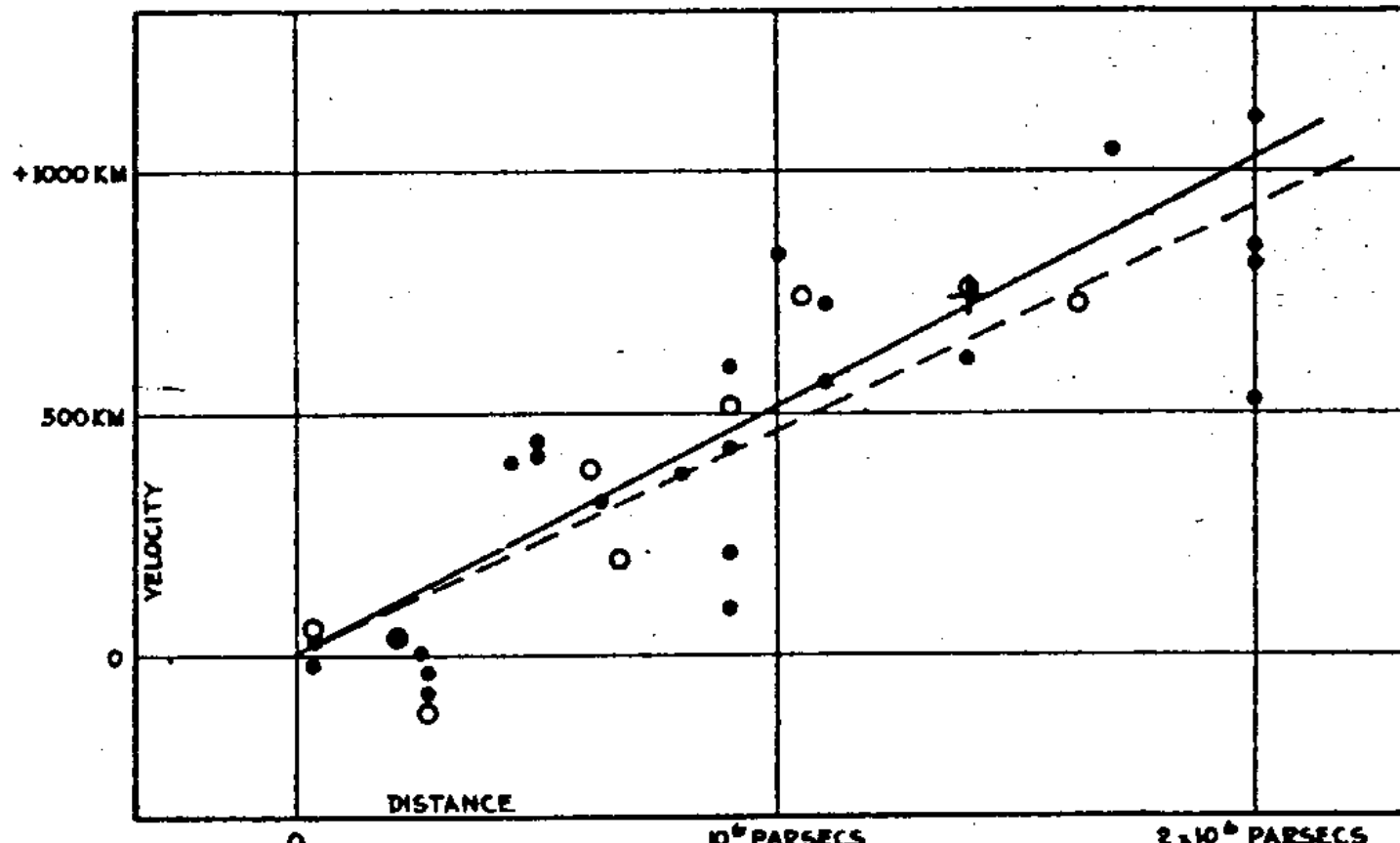


FIGURE 1

Hubble (1936)